Effect of translational and angular momentum conservation on energy equipartition in microcanonical equilibrium in small clusters

Tomoaki Niiyama, Yasushi Shimizu, Taizo R. Kobayashi, Teruaki Okushima, and Kensuke S. Ikeda*
Department of Physics, Ritsumeikan University, Noji-higashi 1-1-1, Kusatsu 525-8577, Japan
(Received 18 December 2008; published 1 May 2009)

We investigate numerically and analytically the effects of conservation of total translational and angular momentum on the distribution of kinetic energy among particles in microcanonical particle systems with small number of degrees of freedom, specifically microclusters. Molecular dynamics simulations of microclusters with constant total energy and momenta, using Lennard-Jones, Morse, and Coulomb plus Born-Mayer-type potentials, show that the distribution of kinetic energy among particles can be inhomogeneous and depend on particle mass and position even in thermal equilibrium. Statistical analysis using a microcanonical measure taking into account of the additional conserved quantities gives theoretical expressions for kinetic energy as a function of the mass and position of a particle with only $O(1/N^2)$ deviation from the Maxwell-Boltzmann distribution. These expressions fit numerical results well. Finally, we propose an intuitive interpretation for the inhomogeneity of the kinetic energy distributions.

DOI: 10.1103/PhysRevE.79.051101 PACS number(s): 05.20.Gg, 36.40.Qv, 36.40.Sx

I. INTRODUCTION

Theoretical approaches based on statistical mechanics are believed to work well in the thermodynamic limit in which the number of particles N composing the system is infinitely large. However, in *systems consisting of small numbers of atoms*, such as microclusters, molecules, proteins, and other finite size systems, the traditional view of statistical physics might be significantly modified.

Indeed, several interesting phenomena peculiar to small systems have been reported experimentally and theoretically. For example, in microclusters, reduced melting temperatures [1], anomalous structural fluctuation (of Au cluster) [2–6], negative heat capacity [7–9], rapid alloying phenomenon [10–14], and coexistence of liquid and solid phases [15–17] have been reported, and these phenomena are considered to be manifestations of small number effects.

All physical systems are in contact with an environment which can work as a heat bath. Therefore, all physical systems in thermal equilibrium should be considered to form canonical ensembles. However, there are many systems which can be treated as isolated systems rather than as systems in close contact with thermal environments. In particular, systems consisting of relatively small number of atoms can be often considered as isolated systems. Indeed, many theoretical studies for dynamical and static characteristics of such systems have been done by using Newton's equation of motion for small number of atoms supposing that the system is isolated (the so-called microcanonical simulation) [13–15,18,19]. Unimolecular reactions in gas phase, which have been investigated in fundamental studies of chemical reactions, also have been treated as isolated systems in theoretical and numerical investigations.

If the isolated system is ergodic it forms a microcanonical ensemble with conserved total energy. Under general conditions, the isolated systems conserve total translational and angular momentum in addition to the total energy. This type of systems is also called *EJ ensembles*, and some researchers have investigated them from the viewpoint of Monte Carlo sampling of EJ ensemble phase space and developed techniques for such sampling [20–22].

In bulk material systems consisting of a huge number of atoms, the effect of the additional conserved quantities can be ignored because of the largeness of the number of degrees of freedom. However, the effect of additional conserved quantities might be significant in systems with small number of degrees of freedom. The effect of additional conserved quantities is also an important problem from the viewpoint of dynamical theory of Hamiltonian systems with multiple degrees of freedom.

In this paper, we study the effect of translational and angular momentum conservation on energy equipartition in microcanonical equilibrium in small clusters. This problem is representative of the general effect of conserved quantities on energy equipartition in microcanonical equilibrium. For this purpose, we introduce a theoretical model for microclusters of atoms (or nanoparticles) which captures the essential features of this effect. First, in a molecular dynamics (MD) simulation supposing the conservation of total translational and angular momentum, it is shown that the atoms composing a cluster can have significantly different average kinetic energy. Next, taking the conservation of total translational and angular momentum into account and based on microcanonical ensemble, we derive general formula for the arbitrary order moment of kinetic energy possessed by each individual atom and prove that the velocity distribution of each individual atom obeys the Maxwell-Boltzmann (MB) distribution with its own temperature. These are the main results of the present paper. Finally, the numerical and analytical results are compared and an excellent agreement between them is confirmed.

The main results mentioned above were reported in our preliminary letter [23], however detailed investigations were not presented there because of the limit of pages. The aim of the present paper is to provide the full details of the numerical and analytical investigations.

*ni-yama@ike-dyn.ritsumei.ac.jp

The organization of the present paper is as follows: in Sec. II, we introduce a theoretical model for microclusters of atoms and show that kinetic energy of each atom becomes inhomogeneous with numerical experiments in typical clusters which have Lennard-Jones, Morse, or Coulomb plus Born-Mayer-type potentials even if the systems are in equilibrium. For this, the kinetic energies distributed to each atom and their distributions are calculated with MD. A relation between the kinetic energy distributed to each atom and the atom's mass or the distance from the center of mass is also investigated. From the relation, we show the trend that an atom which is heavier or further from the center of mass possesses less kinetic energy.

In Sec. III, the average kinetic energy of an atom is described as a function of the position and mass of the atom from analytical estimation of the energy using a microcanonical measure. The expression for higher-order moments of the kinetic energy of an atom and its distribution function are also derived. And we show that the distribution function fits a MB distribution whose parameter is the local temperature corresponding to the atom.

Finally, we compare numerical results of Sec. II and the theoretical estimation of Sec. III and argue that the inhomogeneity of local temperature is caused by conservation of the total translational and angular momentum of the cluster in Sec. IV.

II. NUMERICAL EXPERIMENTS

In this section we present results of MD experiments on the distribution of kinetic energy in small clusters and characterization in terms of local temperature.

First, let us consider the temperature of an isolated system which consists of N particles in the three-dimensional space. If we suppose that the system is ergodic and is described by a microcanonical ensemble, the statistics of any arbitrarily chosen subsystem should obey a canonical ensemble in the thermodynamic limit. Since any particle ℓ forms a subsystem, the distribution of its kinetic energy κ_ℓ should rigorously obey the MB distribution function with the *single common temperature* T,

$$\rho(\kappa_\ell) \propto \sqrt{\kappa_\ell} e^{-\kappa_\ell/k_B T}. \tag{1}$$

Here T is the temperature defined for the whole system on the basis of Boltzmann's entropy $S(E)$,

$$\frac{1}{T} = \frac{dS(E)}{dE}. \tag{2}$$

This is a textbook matter of statistical mechanics. This result, however, holds in the limit of $N \gg 1$. For a small isolated system like a microcluster, the above argument might not hold.

As we shall show below, the velocity distribution is well fitted by the Maxwell-Boltzmann distribution,

$$\rho(\kappa_\ell) \propto \sqrt{\kappa_\ell} e^{-\kappa_\ell/k_B T_\ell^{\mathrm{MB}}}. \tag{3}$$

However, if the system is small enough, the effective temperature T_ℓ^{MB} in general differs depending on the position and mass of the atom. We call T_ℓ^{MB} the local MB temperature. A more easily computable temperaturelike parameter of the individual atom is the effective temperature of the kinetic energy distributed to the atom ℓ, which we call local kinetic temperature,

$$T_\ell^{\kappa} = \frac{2\langle \kappa_\ell \rangle}{3k_B}. \tag{4}$$

In the following, we generically call these temperatures T_ℓ^{MB} and T_ℓ^{κ} as *local temperatures*. These local temperatures are introduced in analogy with the kinetic temperature of the cluster which is widely used in MD or Monte Carlo simulations (for example, see Refs. [19,24]) defined by

$$T_K = \frac{2\langle K \rangle}{(3N-6)k_B}, \tag{5}$$

where $\langle K \rangle$ is average total kinetic energy. Later theoretical consideration will lead us to a justification of this definition of kinetic temperature as the temperature based on the Boltzmann entropy (see Sec. III E). The above definitions of temperature were also studied by Jellinek and Goldberg [25] or Salian [26].

The numerical evidence for inhomogeneity of the local temperature in microclusters will be fully discussed in Sec. II C. The local temperature distribution is homogeneous if total translational and angular momentum are not conserved due to application of an asymmetric external perturbation. Thus we conclude that the inhomogeneity is caused by the additional conserved quantities.

We first discuss details of the setting of numerical experiments.

A. Models

Many types of empirical atomic interaction potentials have been used for MD simulation of various materials, including microclusters. The type of such a potential usually affects the dynamical or statistical properties of the system. In order to investigate universal properties of microclusters, we examine three well-known two body model potentials, namely, the Lennard-Jones (LJ) potential, the Morse potential, and the Coulomb plus Born-Mayer (C+BM) potential.

The above three potentials are well known as simple models of rare gas, metals, and alkali halide crystals, respectively, and they represent various types of atomic interaction of short, medium, and Coulomb long range forces. The clusters which form with these potentials take various structures, e.g., icosahedral or cubic (rocksalt) structure [27,28]. In addition, alkali halide clusters have another feature that the clusters are composed of atoms with different masses. As shown in later sections, this feature plays a particularly important role.

For the LJ potential [29] given by

$$v_{kl}^{\mathrm{LJ}}(r_{ij}) = 4\epsilon_{kl}\left\{\left(\frac{\sigma_{kl}}{r_{ij}}\right)^{12} - \left(\frac{\sigma_{kl}}{r_{ij}}\right)^{6}\right\}, \tag{6}$$

the argon parameters ϵ_{kl}=0.0104 eV and σ_{kl}=3.40 Å were used, where r_{ij} is the distance between ith and jth atoms. For the Morse potential [30],

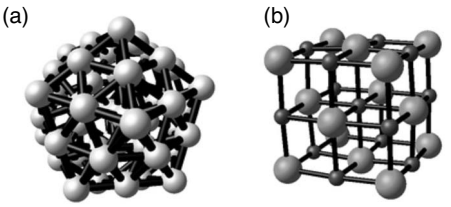

FIG. 1. Initial configurations of the clusters. (a) $(Ar)_{55}$ and $(Cu)_{55}$ (icosahedral structure). (b) $(NaI)_{13}I^-$ ($3\times3\times3$ cubic structure, $N=27$). Small sphere: Na^+; large sphere: I^-.

$$v_{kl}^{M}(r_{ij}) = \epsilon_{kl}\{e^{-2\beta(r_{ij}-\sigma)} - 2e^{-\beta(r_{ij}-\sigma)}\}, \tag{7}$$

the copper parameters $\epsilon_{kl}=0.3429$, $\beta=1.358$ Å^{-1}, and $\sigma=2.866$ Å were adopted [31]. And for C+BM potential [32],

$$v_{kl}^{\mathrm{CBM}}(r_{ij}) = \frac{q_k q_l}{r_{ij}} + A_{kl}\exp\left(\frac{R_k + R_l - r_{ij}}{\rho_{kl}}\right), \tag{8}$$

where q_i is the charge on ion i, A_{ij} and ρ_{kl} are parameters which we chose to be Tosi-Fumi parameters [33,34] for sodium iodine (NaI). We further note that the mass of I^- ion is 5.5 times as heavy as that of Na^+ ion. Because of the above choice of parameters, in this paper we refer to a cluster with LJ, Morse, or C+BM potential as Ar cluster, Cu cluster, and NaI cluster, respectively, and represent them as $(Ar)_N$, $(Cu)_N$, and $(NaI)_n$, respectively, where N is the number of atoms and n is the number of cation-anion pairs.

Employing the model potentials defined above, the model Hamiltonian of a cluster is described as

$$H(\boldsymbol{p},\boldsymbol{q}) = \sum_{i=1}^{N}\frac{\boldsymbol{p}_i^2}{2m_i} + \sum_{i<j}^{N} v_{kl}(r_{ij}) + U(\boldsymbol{q}), \tag{9}$$

where $\boldsymbol{p}_i$ and $\boldsymbol{q}_i$ are ith atom's momentum and coordinate vector and m_i is the mass of the ith atom, respectively. The extra potential $U(\boldsymbol{q})$ represents an external force breaking translational and rotational symmetries, which is applied in order to investigate the role of conserved quantities in the inhomogeneous temperature distribution. This potential is only used in Sec. II E; in other sections the external potential is omitted so translational and rotational symmetries are maintained.

B. Initial configurations

In this paper, we consider clusters with close-packed configurations as initial configurations and relatively low temperatures such that atoms do not change their original sites. This allows an evaluation of local temperature and its dependence on position. Moreover, three moments of inertia around principal axes of the cluster are nearly equal. Such a symmetry allows us to interpret the numerical results in later sections more easily.

We choose a cubic rocksalt-type structure as the initial configuration of $(NaI)_n$ clusters and icosahedral structures for $(Ar)_N$ and $(Cu)_N$. These initial configurations, icosahedral and cubic structure, are shown in Fig. 1 [the center of the $(NaI)_n$ is occupied by a Na^+ atom].

In case of rocksalt $(NaI)_n$ clusters the directions of principal axes of the cluster are $\langle 100\rangle$, $\langle 010\rangle$, and $\langle 001\rangle$ directions and equivalent if we neglect thermal atomic vibration. For $(Cu)_N$ or $(Ar)_N$, icosahedral structure of the clusters has three different moments of inertia, but the differences are no more than 10%, so we can regard $I_x \simeq I_y \simeq I_z$.

C. Numerical method to evaluate local temperature

With the initial configurations of isolated clusters presented above we executed MD simulation by solving Hamilton's equation of motion and evaluated kinetic energies of each atom. Details of the procedure for the evaluation are described below.

To prepare stable initial configurations, we applied the steepest decent algorithm, with which the system reaches a local minimum on its potential energy surface, which corresponds to a stable structure. Without any external forces breaking translational and rotational symmetries, all the components of total translational and angular momentum are conserved. To avoid complications due to the presence of these conserved quantities, we executed the MD simulation under the null total translational and angular momentum condition. To prepare this null momenta initial condition, we slightly distorted the stable structure by moving each atom at random from its equilibrium position and set initial velocity of each atom to zero. This initial configuration distorted from the equilibrium position causes internal vibrational motion, but the initial total translational and angular momentum are zero at the initial time. So the momenta vanish throughout the MD simulation because of the conservation of the total translational and angular momentum.

To control the total kinetic energy of the system, we employ the velocity scaling method with which the total kinetic energy is increased or decreased in order to achieve the desired value. (The velocity scaling method should be done under the constraint of total translational and angular momentum conservation.) After achieving the desired total kinetic energy, the cluster is evolved according to Hamilton's equation of motion for some period (typically 10 ns) until the system relaxes to thermal equilibrium. Eigenfrequencies of clusters in our study are approximately $1\times10^{-1}-1$ ps, so the atoms can vibrate about 10^4-10^5 times during this relaxation time. Thus we can consider the time is long enough for the system to reach equilibrium.

Then various quantities such as kinetic energy κ_ℓ of each atom (ℓ specifies each atom), its distance from the center of the cluster r_ℓ, and so on are sampled at appropriate interval $\Delta\tau$. Using all these quantities, we compute the time averaged kinetic energy $\langle\kappa_\ell\rangle$ of each atom, its distribution $\rho(\kappa_\ell)$, the averaged distances from the center of the cluster $\langle r_\ell\rangle$, and the average moments of inertia $\langle I_x\rangle$, $\langle I_y\rangle$, and $\langle I_z\rangle$. To solve Hamilton's equation of motion, we employed the velocity form of the Verlet algorithm, where the time steps used were typically 10 fs for $(Ar)_N$ and $(NaI)_n$ clusters and 1 fs for $(Cu)_N$ cluster. (Numerical accuracy is much improved if one employs a higher-order symplectic integrator; the Verlet algorithm is equivalent to the second-order symplectic integrator.)

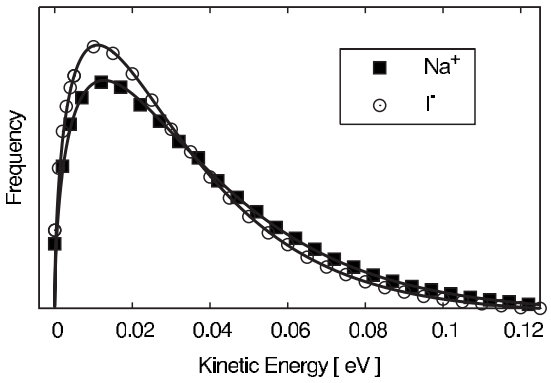

FIG. 2. The frequency distributions of the kinetic energy of the Na^+ atom (solid circles) at the center and the I^- atom (white circles) at a vertex of $(NaI)_{13}I^-$ cluster and the corresponding theoretical curves of MB distributions.

D. Local temperature with vanishing total translation and angular momentum

In this section, we evaluate local temperature T_ℓ^{MB} of each atom in the cluster models introduced in Sec. II A and investigate the relation between the local temperature and position or mass of the atom based on the MD simulation whose procedure is also described in Sec. II C. It is note that we chose the temperature of clusters to be lower than melting temperature, so no melting, much less evaporation, was observed during any of the numerical experiments described below.

First, we examined the isolated $(NaI)_{13}I^-$ cluster whose total translational and angular momentum are conserved. In this simulation, the total energy was -3.122 eV/atom which corresponds to $T_K \simeq 300$ K, where the total simulation time and the sampling interval were taken as $\tau = 100$ ns and $\Delta\tau = 100$ fs, respectively. From the numerical experiment, the average moment of inertia of the cluster was calculated: $\langle I \rangle \simeq 2.89 \times 10^4$ u Å^2.

In Fig. 2, the distributions of kinetic energy are depicted and compared with the Maxwell-Boltzmann distribution function fitted by the least-squares method. The solid circles in the figure represent the distribution of the kinetic energy of the Na^+ atom at the center of the cluster and the white circles represent the energy of the I^- atom at a vertex of the cluster. The figure shows that these kinetic energy distributions fit the MB distribution very well, but the energy distributions at the two sites differ significantly. This means the temperatures T_ℓ^{MB} determined by fitting to the Maxwell-Boltzmann distribution at the two sites differ significantly, although the Na^+ and I^- atoms belong to the same system.

TABLE I. The local temperatures and distances from the center of mass in the $(NaI)_{13}I^-$ cluster at about 300 K, where r_ℓ, T_ℓ^{MB}, T_ℓ^{κ}, and $\langle \kappa_\ell \rangle$ are the distance from the center of mass, local MB temperature, local kinetic temperature, and average kinetic energy of an atom, respectively.

	$\langle r_\ell \rangle$ (Å)	T_ℓ^{MB} (K)	T_ℓ^{κ} (K)	$\langle \kappa_\ell \rangle$ (eV/atom)
Na^+	0.0	295.2	295.5	0.0381
	4.4	291.8	292.0	0.0332
I^-	3.3	272.0	272.7	0.0352
	5.3	256.4	257.4	0.0332

The local MB temperatures T_ℓ^{MB}, the local kinetic temperatures T_ℓ^{κ}, and the average kinetic energy $\langle \kappa_\ell \rangle$ of individual atoms are shown in Table I for four types of atoms taken from the cluster: the first kind of atom is the Na^+ atom at the center of the cluster, the second and third are a nearest neighbor (I^- atom, $\langle r_\ell \rangle = 3.3$ Å) and a second nearest neighbor (Na^+ atom, $\langle r_\ell \rangle = 4.4$ Å) from the center, respectively, and the fourth kind of atom is one of the atoms on a vertex of the cluster (I^- atoms, $\langle r_\ell \rangle = 5.3$ Å).

Because of the symmetrical structure, these four types of atoms represent all the atoms in the cluster. From the Table I, both temperatures, T_ℓ^{MB} and T_ℓ^{κ}, agree quite well within 1%. This agreement provides another evidence that the kinetic energy distributions of each atom agree with the MB distribution. Moreover, this excellent agreement strongly suggests that, in spite of the smallness of the number of constituent atoms ($N = 27$), each sampled atom is in thermal equilibrium and the rest of the whole system operates as a heat reservoir with well defined temperature (Salian [26] showed that a system containing only four atoms works as a heat reservoir).

However, a surprising fact is that the temperatures of the different types are different although every atom is in equilibrium with the common system, namely, the whole cluster, and the maximum difference is as large as 15% (Table I).

The local temperatures of each atom of the $(NaI)_{13}I^-$ cluster are plotted in Fig. 3(a) as a function of the average distance $\langle r_\ell \rangle$ from the center of mass. One can recognize only four plots in the figure. This is because the atoms at the same

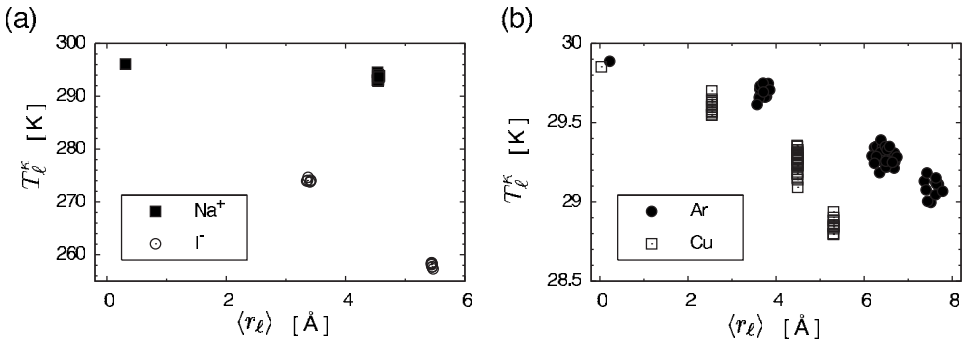

FIG. 3. The local temperature T_ℓ^{κ} of each individual atom as a function of the average distance from the center of mass $\langle r_\ell \rangle$ in $(NaI)_{13}I^-$, Cu_{55}, and Ar_{55}. (a) The local temperature of the $(NaI)_{13}I^-$ cluster. Solid squares and white circles are the temperature of Na^+ and I^- atoms, respectively. (b) The local temperature in Cu_{55} (white squares) and Ar_{55} (black circles) clusters.

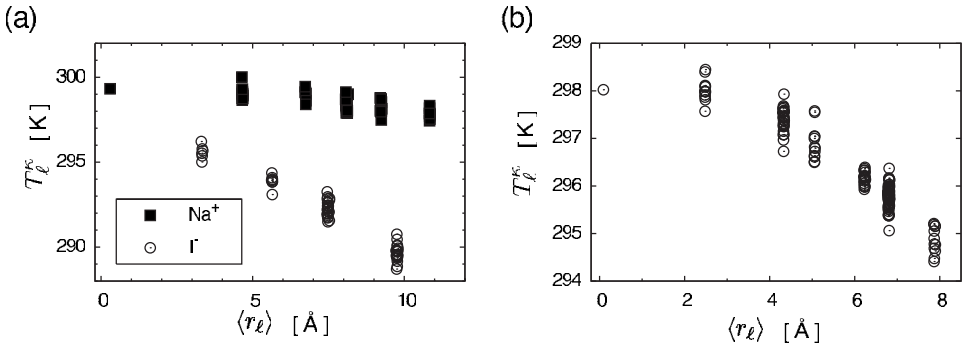

FIG. 4. The local temperature T_ℓ^κ of each individual atom as a function of the average distance from the center of mass $\langle r_\ell \rangle$ in clusters consisting of many atoms. (a) $(NaI)_{62}I^-$ ($N=125$). (b) Cu_{147} ($N=147$).

distance from the center have the same local temperature.

Moreover, it should be noticed that the plots of Na^+ are systematically higher than the plots of I^-, which strongly suggests a mass dependence of local temperature.

The results of numerical experiments with Ar_{55} and Cu_{55} clusters that are bounded by atomic interaction different from $(NaI)_{13}I^-$ are shown in Fig. 3(b). The kinetic temperature was adjusted to $T_K \simeq 30$ K, which is less than the melting temperature of argon cluster, and the average moments of inertia of Ar_{55} and Cu_{55} are 5.46×10^4 and 4.24×10^4 u Å^2, respectively. The maximum local temperature difference is only about 3%, but the figure also shows that the local temperatures decrease as the distance of the atom from the center of the cluster increases and the heavier particles have lower local temperatures.

Moreover, comparison of Figs. 3(a) and 3(b) also shows that the heavier particles have lower local temperatures than lighter ones since the mass of Na^+ is smaller than I^- and the mass of Ar is smaller than Cu.

Next, we investigate dependence of local temperature upon size of cluster or the total number of atoms contained in the clusters. For this purpose, we carried out numerical experiments for $(NaI)_{62}I^-$ ($5 \times 5 \times 5$ cubic structure; $N=125$) and Cu_{147} (icosahedral structure) clusters. The simulation interval and the temperature were taken as $\tau=100$ ns and $T_K \simeq 300$ K. From the numerical results, the average moments of inertia of $(NaI)_{62}I^-$ and Cu_{147} were 3.89×10^5 and 2.18×10^5 u Å^2, respectively.

The local temperatures in the clusters are plotted against distance from the center of mass in Fig. 4. The results for $(NaI)_{62}I^-$ and Cu_{147} clusters are shown in Figs. 4(a) and 4(b), respectively. Maximum difference among the local temperatures is significantly reduced; it is only about 3% for $\{\boldsymbol{e}_4, \boldsymbol{e}_5, \boldsymbol{e}_6\}$ and it is 1% for Cu_{147} cluster.

Thus, we can conjecture that the distribution of local temperatures over the atoms is not in general homogeneous in an isolated small cluster but the inhomogeneity disappears as the cluster size increases.

In a given cluster the local temperature defined for an individual atom is lower for atoms at sites more distant from the center or for atoms with heavier mass, but inhomogeneity in the local temperature distribution disappears when the number of atoms in the cluster becomes large.

E. Local temperature with nonvanishing total translational and angular momentum

In the above numerical simulation, the system has conserved quantities, namely, total translational and angular momentum, due to the spatial symmetry in the system. One possibility is that the presence of conserved quantities may modify the equilibrium condition significantly in small systems. If this is the case, we can conjecture that the temperature distribution will recover homogeneity when any external force breaking the spatial symmetry is applied.

To confirm this conjecture we investigated a system for which the total translational and angular momentum are not conserved due to the application of an asymmetric external perturbation represented by an asymmetric harmonic trap potential $U(x,y,z)=\epsilon_{xx}x^2+\epsilon_{yy}y^2+\epsilon_{zz}z^2$, where ϵ_{xx}, ϵ_{yy}, and ϵ_{zz} are constant parameters of the potential and the trap is asymmetrical when these parameters are not equal. We note that when such an external potential is applied to a cluster, the whole system including the external potential can still be regarded as an isolated system.

We took $(NaI)_{13}I^-$ cluster for this examination and put the cluster in the trap potential with the parameters $\epsilon_{xx}=0.5 \times 10^{-2}$, $\epsilon_{yy}=1.0 \times 10^{-2}$, and $\epsilon_{zz}=0.7 \times 10^{-2}$. The interval of the simulation using the same procedure mentioned above was $\tau=1$ μs and the temperature $T_K \simeq 300$ K.

The local temperatures are shown in Fig. 5 as a function of distance from the center of mass. Rigorously a very slight difference among the local temperatures still remains but is only about a few degrees at the maximum, which is much less than the maximum difference without the trap [about 40 K in Fig. 3(a)]. Disappearance of the temperature difference was confirmed also in Cu and Ar clusters which have different types of interaction.

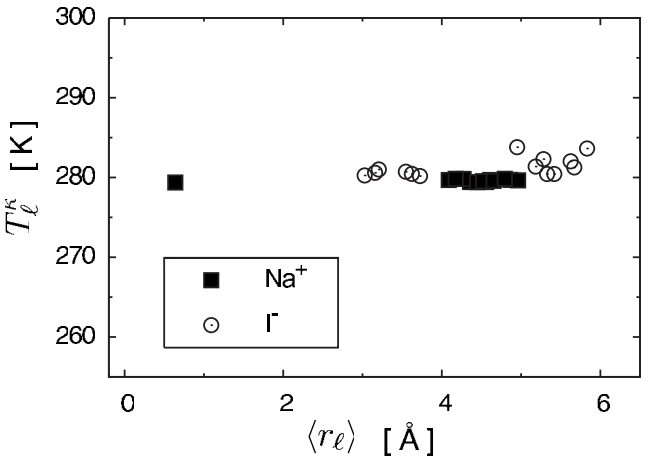

FIG. 5. The local temperature T_ℓ^κ of each individual atom as a function of the average distance from the center of mass $\langle r_\ell \rangle$ for the $(NaI)_{13}I^-$ cluster trapped in an asymmetrical harmonic potential.

These results strongly support our conjecture that the conservation of total translational and angular momentum results in inhomogeneity of local temperature distribution in isolated clusters.

III. THEORETICAL ANALYSIS

In this section we evaluate the local temperature based on statistical mechanics using microcanonical invariant measure with conserved total translational and angular momentum. The final aim of this section is to derive a rigorous formula for the moment of local kinetic energy () and an approximate distribution function for the local kinetic energy under the constraint of total translational and angular momentum conservation (). All the results are expressed as average with respect to the coordinate variables which represent the position dependency explicitly.

We suppose that the system is ergodic and the long time average of physical quantities can be replaced by the phase space average with respect to the microcanonical invariant measure with fixed angular momentum $\boldsymbol{q}$ and fixed total translational momentum $\boldsymbol{P}_0$,

$$\rho(\boldsymbol{q},\boldsymbol{p}) = \mathcal{N}\delta[H(\boldsymbol{q},\boldsymbol{p}) - E]\delta(\boldsymbol{L} - \boldsymbol{L}_0)\,\delta(\boldsymbol{P} - \boldsymbol{P}_0), \qquad (10)$$

where $\mathcal{N}$ is the normalization constant and E is total energy of the system [35]. Here we use the mass-weighted coordinate and momentum $(\boldsymbol{q}_i,\boldsymbol{p}_i)=(\sqrt{m_i}\tilde{\boldsymbol{q}}_i,\tilde{\boldsymbol{p}}_i/\sqrt{m_i})$, where $\tilde{\boldsymbol{q}}_i$ and $\tilde{\boldsymbol{p}}_i$ are the coordinate and momentum of ith atom in original coordinate before transforming to mass-weighted coordinate, i.e., these vectors correspond to the vectors $\boldsymbol{q}_i$ and $\boldsymbol{p}_i$ in Eq. (9), respectively. (Although this notation may cause some confusion, we employ it for simplicity in descriptions below.) So the Hamiltonian is given as

$$H(\boldsymbol{p},\boldsymbol{q}) = \sum_{i=1}^{N} \frac{\boldsymbol{p}_i^2}{2} + V(\boldsymbol{q}_1,\boldsymbol{q}_2,\ldots,\boldsymbol{q}_N), \qquad (11)$$

and the total translational and angular momentum are

$$\boldsymbol{P} = \sum_{i=1}^{N} \sqrt{m_i}\boldsymbol{p}_i, \quad \boldsymbol{L} = \sum_{i=1}^{N} \boldsymbol{q}_i \times \boldsymbol{p}_i, \qquad (12)$$

respectively, where $\boldsymbol{q}_i$ and $\boldsymbol{p}_i$ are the coordinate and momentum of ith atom and N is the number of atoms in the system. For the sake of simplicity, we set $\boldsymbol{L}_0=0$ and $\boldsymbol{P}_0=0$ in the sections below.

A. Collective momentum variables

We represent the whole system by the $3N$-dimensional coordinate and momentum vectors $\boldsymbol{q}$ and $\boldsymbol{p}$, respectively,

$$\boldsymbol{q} = {}^t(q_{1x},q_{1y},q_{1z},\ldots,q_{Nz}),$$

$$\boldsymbol{p} = {}^t(p_{1x},p_{1y},p_{1z},\ldots,p_{Nz}).$$

By using the microcanonical invariant measure the phase space average of arbitrary physical quantity $X(\boldsymbol{q},\boldsymbol{p})$ is

$$\langle X(\boldsymbol{q},\boldsymbol{p})\rangle = \frac{\int X(\boldsymbol{q},\boldsymbol{p})\rho(\boldsymbol{q},\boldsymbol{p})d\boldsymbol{q}d\boldsymbol{p}}{\int \rho(\boldsymbol{q},\boldsymbol{p})d\boldsymbol{q}d\boldsymbol{p}}. \qquad (13)$$

The integration over the variables $\boldsymbol{q}$ and $\boldsymbol{p}$ is done in the following way. We first fix the coordinate variables $\boldsymbol{q}$, then integrate over the momentum variables $\boldsymbol{p}$, and next integration over $\boldsymbol{q}$ is carried out. While carrying out the integration over the momentum variables $\boldsymbol{p}$, the constraint $\boldsymbol{L}=0$ and $\boldsymbol{P}=0$ must be fully taken into account. For this purpose, it is convenient to introduce collective variables associated with the total translational and angular momentum, supposing that the coordinate variables $\boldsymbol{q}$ are temporally fixed. We first move to the frame which is taken as the principal axes of the moment of inertia with the origin at the center of mass. We call such a frame *principal frame*. Therefore the coordinate variables in the frame can be treated as a function of the variables in the original frame, $\boldsymbol{q}'=\boldsymbol{q}'(\boldsymbol{q})$. In the principal frame the coordinate and momentum vectors are represented by

$$\boldsymbol{q}' = {}^t(q'_{1x},q'_{1y},q'_{1z},\ldots,q'_{Nx},q'_{Ny},q'_{Nz}),$$

$$\boldsymbol{p}' = {}^t(p'_{1x},p'_{1y},p'_{1z},\ldots,p'_{Nx},p'_{Ny},p'_{Nz}),$$

and we explicitly distinguish them from $\boldsymbol{q}$ and $\boldsymbol{p}$.

Here we introduce an orthogonal transformation $\boldsymbol{T}(\boldsymbol{q}')$ which can transform into collective momentum and other variables supposing that the coordinate vector $\boldsymbol{q}'$ is fixed. The transformation $\boldsymbol{T}(\boldsymbol{q}')$ is a $3N\times 3N$ orthogonal matrix composed of $3N$ vectors $\{\boldsymbol{e}_i\}$ as orthogonal basis, namely, $\boldsymbol{T}=(\boldsymbol{e}_1,\boldsymbol{e}_2,\ldots,\boldsymbol{e}_{3N})$. It is defined such that the first six variables of the transformed momenta $\boldsymbol{\xi}={}^t\boldsymbol{T}\boldsymbol{p}'$ form the three components of total momentum and the three components of total angular momentum, that is, ${}^t(\xi_1,\xi_2,\xi_3)={}^t(\boldsymbol{e}_1,\boldsymbol{e}_2,\boldsymbol{e}_3)\boldsymbol{p}' = {}^t(P'_x,P'_y,P'_z)/\sqrt{M}$ and ${}^t(\xi_4,\xi_5,\xi_6)={}^t(\boldsymbol{e}_4,\boldsymbol{e}_5,\boldsymbol{e}_6)\boldsymbol{p}' = {}^t(\frac{L'_x}{\sqrt{I_x}},\frac{L'_y}{\sqrt{I_y}},\frac{L'_z}{\sqrt{I_z}})$ (the primes indicate the coordinate in the principal frame), where M and I_α are total mass, $M=\Sigma_i^N m_i$, and inertia moment of the cluster $I_\alpha=\Sigma_i^N(q'^2_{i\beta}+q'^2_{i\gamma})$, respectively, where (α,β,γ) are cyclic permutation of (x,y,z). Thus $\{\boldsymbol{e}_1,\ldots,\boldsymbol{e}_6\}$ must be

$$\boldsymbol{e}_1 = {}^t(\sqrt{m_1},0,0,\ldots,\sqrt{m_N},0,0)/\sqrt{M},$$

$$\boldsymbol{e}_2 = {}^t(0,\sqrt{m_1},0,\ldots,0,\sqrt{m_N},0)/\sqrt{M},$$

$$\boldsymbol{e}_3 = {}^t(0,0,\sqrt{m_1},\ldots,0,0,\sqrt{m_N})/\sqrt{M},$$

$$\boldsymbol{e}_4 = {}^t(0,-q'_{1z},q'_{1y},\ldots,0,-q'_{Nz},q'_{Ny})/\sqrt{I_x},$$

$$\boldsymbol{e}_5 = {}^t(q'_{1z},0,-q'_{1x},\ldots,q'_{Nz},0,-q'_{Nx})/\sqrt{I_y},$$

$$\boldsymbol{e}_6 = {}^t(-q'_{1y},q'_{1x},0,\ldots,-q'_{Ny},q'_{Nx},0)/\sqrt{I_z},$$

respectively. These vectors are normalized by M and I_α. $\{\boldsymbol{e}_1,\boldsymbol{e}_2,\boldsymbol{e}_3\}$ are obviously orthogonal with each other. A vector in $\{\boldsymbol{e}_1,\boldsymbol{e}_2,\boldsymbol{e}_3\}$ and a vector in $\{\boldsymbol{e}_4,\boldsymbol{e}_5,\boldsymbol{e}_6\}$ are also orthogonal because the inner product gives a component of the position of the center of mass. The inner product between two different vectors in $\{\boldsymbol{e}_4,\boldsymbol{e}_5,\boldsymbol{e}_6\}$ is proportional to an off-diagonal element of the inertia tensor, and so it vanishes. It is obvious that all the vectors are normalized to unity, thus all the six vectors are unit orthogonal vectors. This type of transformation was also introduced by other researchers (for instance, see the appendix of Ref. [28]).

Here we consider the unit orthonormal vectors $\{\boldsymbol{a}_j\}$ $(1 \le j \le 3N)$ with all components zero except for the jth element which is 1. These obviously form a normalized set. With these vectors we can construct the undetermined unit orthogonal vectors $\{\boldsymbol{e}_j\}$ for $j \ge 7$ as

$$\boldsymbol{e}_i = \left(\boldsymbol{a}_i - \sum_{k=1}^{i-1} (\boldsymbol{a}_i \boldsymbol{e}_k)\boldsymbol{e}_k \right) \Big/ \left| \boldsymbol{a}_i - \sum_{k=1}^{i-1} (\boldsymbol{a}_i \boldsymbol{e}_k)\boldsymbol{e}_k \right|$$

using Gram-Schmidt orthogonalization, and we obtain the explicit form of the transformation matrix $\boldsymbol{T}$ as $T_{ij} = {}^t\boldsymbol{a}_i\, \boldsymbol{e}_j$. Finally it should be remarked that the relation

$$T_{ij} = {}^t\boldsymbol{e}_i\, \boldsymbol{e}_j = 0 \quad (7 \le i < j \le 3N) \tag{14}$$

holds because these vectors $\boldsymbol{e}_i$ are orthogonal with previous one, $\boldsymbol{e}_j$ $(j<i)$.

B. Statistical average

To investigate local kinetic temperature, it is necessary to evaluate the phase space average of the kinetic energy of one of the atoms which consists of an isolated cluster. For this, we consider, first of all, a formula for the statistical average of an arbitrary physical quantity $X(\boldsymbol{q},\boldsymbol{p})$ which is invariant under spatial rotation of the momentum vectors of individual atoms.

Before evaluating the statistical average [Eq. (13)], we introduce entropy and thermodynamic temperature. We choose the phase space volume enclosed by the equienergy surface as the basis for entropy. Taking into account the constraints $\boldsymbol{L}_0=0$ and $\boldsymbol{P}_0=0$, the phase space volume is

$$\Omega(E) = \int d\boldsymbol{q} d\boldsymbol{p}\, \delta(\boldsymbol{L})\, \delta(\boldsymbol{P})\, \theta[E - H(\boldsymbol{q},\boldsymbol{p})], \tag{15}$$

where $\theta(x)$ is step function. An alternative basis for entropy is the area of the equienergy surface or density of state $d\Omega(E)/dE$, which quantitatively represents the loss of information on the equienergy surface. On the other hand, $\Omega(E)$ is an adiabatic invariant if the system is ergodic, so we think it is a legitimate choice as a basis for entropy. By using $\Omega(E)$, entropy S and temperature T are defined as

$$S = k_B \log\, \Omega(E), \quad T = \Omega'(E)/\Omega(E). \tag{16}$$

(This definition of entropy is not unique. We adopt here the definition based on the adiabatic invariant $\Omega(E)$ [36].)

For evaluating the statistical average [Eq. (13)], we change the reference frame from the rest frame to the principal frame, then the momentum variables $\boldsymbol{p}'$ are split into collective and internal momentum variables with the transformation $\boldsymbol{T}(\boldsymbol{q}')$ introduced in Sec. III A. The momentum represented in the new frame is related to a new variable $\boldsymbol{\xi}$,

$$\boldsymbol{p}' = \boldsymbol{T}(\boldsymbol{q}')\boldsymbol{\xi}. \tag{17}$$

We first carry out the integration over $\boldsymbol{p}$ (or $\boldsymbol{p}'$) by transforming the variables from $\boldsymbol{p}$ to $\boldsymbol{\xi}$ and next complete the integration over the coordinate variables $\boldsymbol{q}$. For the purpose of the present paper, we are allowed to suppose that the quantity $X(\boldsymbol{q},\boldsymbol{p})$ is invariant under the rotation of individual momentum vector, and so $X(\boldsymbol{q},\boldsymbol{p})=X(\boldsymbol{q},\boldsymbol{p}')$. Noticing that $\boldsymbol{P} = \sqrt{M}(\xi_1,\xi_2,\xi_3)$ and $\boldsymbol{L}=(\xi_4\sqrt{I_x},\xi_5\sqrt{I_y},\xi_6\sqrt{I_z})$, Eq. (13) becomes

$$\langle X(\boldsymbol{q},\boldsymbol{p})\rangle = \frac{\int d\boldsymbol{\xi} d\boldsymbol{q} X[\boldsymbol{q},\boldsymbol{T}(\boldsymbol{q})\boldsymbol{\xi}]\sigma(\boldsymbol{\xi},\boldsymbol{q})/\sqrt{|I(\boldsymbol{q})|}}{\int d\boldsymbol{\xi} d\boldsymbol{q} \sigma(\boldsymbol{\xi},\boldsymbol{q})/\sqrt{|I(\boldsymbol{q})|}}, \tag{18}$$

where $\sigma(\boldsymbol{\xi},\boldsymbol{q}) = \Pi_{i=1}^{6}\delta(\xi_i)\delta[E-H(\boldsymbol{q},\boldsymbol{\xi})]$ is reduced measure [22,28,37], and $I(\boldsymbol{q})=I_xI_yI_z$. [Also note that $H(\boldsymbol{q},\boldsymbol{p})=H(\boldsymbol{q},\boldsymbol{\xi})$ because $\boldsymbol{\xi}^2=\boldsymbol{p}'^2=\boldsymbol{p}^2$.]

The above transformation can immediately be applied to compute the phase space volume defined by Eq. (15). Indeed, by using the new variables $\boldsymbol{\xi}$, Eq. (15) is rewritten as

$$\begin{aligned}\Omega(E) &= \int d\boldsymbol{q}/\sqrt{I(\boldsymbol{q})} \int d\boldsymbol{\xi} \prod_{i=1}^{6} \delta(\xi_i)\, \theta[E - H(\boldsymbol{q},\boldsymbol{\xi})] \\ &= \int d\boldsymbol{q}/\sqrt{I(\boldsymbol{q})} \int \prod_{i=7}^{3N} d\xi_i \theta\left[K(E,\boldsymbol{q}) - \sum_{i=7}^{3N} \xi_i^2/2 \right],\end{aligned} \tag{19}$$

where

$$K(E,\boldsymbol{q}) = E - V(\boldsymbol{q}) \tag{20}$$

is the total kinetic energy of the system. Integration over ξ_i in Eq. (19) is nothing more than the volume of the $3N-6$-dimensional hypersphere with the radius $\sqrt{2K(E,\boldsymbol{q})}$, and so we get

$$\Omega(E) = \pi_{3N-6} \int d\boldsymbol{q} [2K(E,\boldsymbol{q})]^{(3N-6)/2}/\sqrt{I(\boldsymbol{q})}, \tag{21}$$

where π_M is the volume of M-dimensional unit hypersphere which is described with the gamma function $\Gamma(z)$: $\pi_M = \pi^{M/2}/\Gamma(M+2/2)$.

The quantity $X(\boldsymbol{q},\boldsymbol{p})$ which we would like to compute contains only the variables associated with one atom (or multiple atoms) in the cluster. In such a case, it contains only a small number of ξ_i variables including the first six variables $\xi_1, \xi_2, \ldots, \xi_6$ as will be shown in Secs. III C–III E. Thus we suppose the quantity X contains only a part of the momentum variables $\boldsymbol{\xi}' \equiv (\xi_1,\xi_2,\ldots,\xi_{6+s})$, where s is an integer $(0 \le s \le 3N)$. Then we can write $X(\boldsymbol{q},\boldsymbol{p})=X(\boldsymbol{q},\boldsymbol{p}')=X(\boldsymbol{q},\boldsymbol{T}\boldsymbol{\xi}')$, and

the integration over the rest of momentum variables $\xi_{7+s},\cdots,\xi_{3N}$ can be executed as follows:

$$\int \delta[E-V(\boldsymbol{q})-\boldsymbol{\xi}^2/2]\prod_{i=7+s}^{3N} d\xi_i$$
$$= \frac{d}{dE}\int \theta\left[K(E-\boldsymbol{\xi}'^2/2,\boldsymbol{q})-\sum_{k=7+s}^{3N}\xi_k^2/2\right]\prod_{i=7+s}^{3N} d\xi_i$$
$$= (3N-6-s)\pi_{3N-6-s}[2K(E-\boldsymbol{\xi}'^2/2,\boldsymbol{q})]^{(3N-8-s)/2}, \tag{22}$$

where we use the fact that the integral in the second term is the volume of a $3N-6-s$-dimensional hypersphere with radius $\sqrt{2K(E-\boldsymbol{\xi}'/2,\boldsymbol{q})}$. Applying this relation in Eq. (18) gives the formula for statistical average,

$$\langle X(\boldsymbol{q},\boldsymbol{p})\rangle = C_{N,s}\frac{\int d\boldsymbol{\xi}' d\boldsymbol{q} X(\boldsymbol{q},\boldsymbol{T}\boldsymbol{\xi}')\hat{\sigma}(\boldsymbol{\xi}',\boldsymbol{q})/\sqrt{|I(\boldsymbol{q})|}}{\int d\boldsymbol{q}[2K(E,\boldsymbol{q})]^{(3N-8)/2}/\sqrt{|I(\boldsymbol{q})|}}. \tag{23}$$

$$\hat{\sigma}(\boldsymbol{\xi}',\boldsymbol{q}) = \prod_{i=1}^{6}\delta(\xi_i)[2K(E-\boldsymbol{\xi}'^2/2,\boldsymbol{q})]^{(3N-8-s)/2}, \tag{24}$$

where

$$C_{N,s} = \frac{3N-6-s}{3N-6}\frac{\pi_{3N-6-s}}{\pi_{3N-6}} \tag{25}$$

and for the denominator integration Eq. (22) with $s=0$ is used. In particular, we can also obtain the statistical average of quantities *depending on only the coordinate* $\boldsymbol{q}$,

$$\langle X(\boldsymbol{q})\rangle = \frac{\int d\boldsymbol{q} X(\boldsymbol{q})[2K(E,\boldsymbol{q})]^{(3N-8)/2}/\sqrt{|I(\boldsymbol{q})|}}{\int d\boldsymbol{q}[2K(E,\boldsymbol{q})]^{(3N-8)/2}/\sqrt{|I(\boldsymbol{q})|}}, \tag{26}$$

by setting $s=0$ and $C_{N,0}=1$ and integrating over $\xi_1,\ldots,\xi_6$. We here remark that the notation $\langle\ \rangle$ often used in the main results of the present paper is the statistical average in the sense of Eq. (26).

As a simple application we examine the moments of the total kinetic energy. Since the total kinetic energy is $\boldsymbol{p}^2/2 = E-V(\boldsymbol{q})=K(E,\boldsymbol{q})$, putting $X(\boldsymbol{q})=K(E,\boldsymbol{q})^D$ and $s=0$ into Eq. (26), we immediately obtain

$$\langle K(E,\boldsymbol{q})^D\rangle = \frac{1}{2^D}\frac{\int d\boldsymbol{q}[2K(E,\boldsymbol{q})]^{(3N-8)/2+D}/\sqrt{I(\boldsymbol{q})}}{\int d\boldsymbol{q}[2K(E,\boldsymbol{q})]^{(3N-8)/2}/\sqrt{I(\boldsymbol{q})}}. \tag{27}$$

Moreover, comparing this and the definition of thermodynamic temperature [Eq. (16)], which is based on the definition of the entropy using the phase volume [Eq. (21)], immediately leads to the result

$$T(E) = \frac{\langle 2K(E,\boldsymbol{q})\rangle}{(3N-6)k_B}. \tag{28}$$

This equation agrees with the conventional microcanonical kinetic temperature [Eq. (5)]. It should be remarked that, if the entropy is defined by the density of state, namely, $S = k_B\log[d\Omega(E)/dE]$, the above relation, which allows the simple physical interpretation that 6 degrees of freedoms are quenched by the conservation law, is subtly modified.

C. Average kinetic energy of a particle

The numerically observed results in this paper suggest that the local kinetic energy is closely connected with the local temperature, and so we first evaluate analytically the average value of kinetic energy $\langle\kappa_\ell\rangle$ of an atom in an isolated cluster. Let us consider the ℓth atom in the cluster. According to the procedure of the statistical average represented by Eq. (18), we first fix $\boldsymbol{q}$ and then calculate the x component of ℓth atom's kinetic energy $\boldsymbol{p}_\ell^2/2=\boldsymbol{p}_\ell'^2/2$ in the principal frame, namely, $p_{\ell x}'^2/2$ by integrating over the new variables $\boldsymbol{\xi}$. Finally the average over the $\boldsymbol{q}$ is taken. We take $p_{\ell x}'$ as the seventh component of the vector $\boldsymbol{p}'$. Because of Eq. (14), the following relation holds:

$$p_{\ell x}' = \sum_{k=1}^{7} T_{7k}\xi_k. \tag{29}$$

Since the average formula [Eq. (23)] with $s=1$ contains $\Pi_{i=1}^6\delta(\xi_i)$, making use of Eq. (29) gives

$$\left\langle\frac{p_{\ell x}'^2}{2}\right\rangle = \frac{C_{N,1}}{2}\frac{\int ({}^t\boldsymbol{a}_7\,\boldsymbol{e}_7)^2\xi_7^2\left[2K\left(E-\frac{\xi_7^2}{2},\boldsymbol{q}\right)\right]^{(3N-9)/2} d\xi_7 d\boldsymbol{q}/\sqrt{|I(\boldsymbol{q})|}}{\int [2K(E,\boldsymbol{q})]^{(3N-8)/2} d\boldsymbol{q}/\sqrt{|I(\boldsymbol{q})|}}. \tag{30}$$

The integration over the momentum variable ξ_7 can easily be done by using the relation

$$C_{N,1}\int \xi_i^2[2(E-\xi_i^2/2-V)]^{(3N-9)/2}d\xi_i = \frac{[2K(E,\boldsymbol{q})]^{(3N-6)/2}}{3N-6}$$

(see Appendix A). Consequently, the statistical average of $p_{\ell x}'^2/2$ reduces to the average over the coordinate variables in the sense of Eq. (26),

$$\left\langle \frac{p_{\ell x}'^2}{2} \right\rangle = \frac{\langle ({}^t\boldsymbol{a}_7\,\boldsymbol{e}_7(\boldsymbol{q}))^2 K(E,\boldsymbol{q})\rangle}{3N-6}. \tag{31}$$

Thus the only information necessary is the $\boldsymbol{q}$ dependence of the vector $\boldsymbol{e}_7$. The vector $\boldsymbol{e}_7$ is constructed according to the Gram-Schmidt procedure so as to be orthogonal to the first six vectors $\boldsymbol{e}_1,\boldsymbol{e}_2,\ldots,\boldsymbol{e}_6$, which leads to

$$({}^t\boldsymbol{a}_7\,\boldsymbol{e}_7)^2 = \left(1-\frac{m_\ell}{M}-\frac{q_{\ell z}'^2}{I_y}-\frac{q_{\ell y}'^2}{I_z}\right). \tag{32}$$

In the above consideration, we took p_7' (the seventh component of $\boldsymbol{p}'$) as the x direction momentum of the ℓth atom $p_{\ell x}'$. The cyclic permutations $(x,y,z)\to(y,z,x)\to(z,x,y)$ allow us to replace p_7 by y and z components of the original momentum vector, which gives the expression for $\langle p_{\ell y}'^2/2\rangle$ and $\langle p_{\ell z}'^2/2\rangle$ corresponding to Eq. (31) with Eq. (32). Therefore, the general expression corresponding to Eq. (32) is

$$\left\langle \frac{p_{\ell\alpha}'^2}{2} \right\rangle = \left\langle \left[1-\frac{m_\ell}{M}-\frac{q_{\ell\beta}'^2}{I_\gamma}-\frac{q_{\ell\gamma}'^2}{I_\beta}\right]\frac{K(E,\boldsymbol{q})}{3N-6}\right\rangle, \tag{33}$$

where α, β, and γ is a cyclic permutation of x, y, and z.

The sum of the three components yields the average kinetic energy of ℓth atom,

$$\langle\kappa_\ell\rangle = \left\langle \left[3-3\frac{m_\ell}{M}-\sum_{\alpha=x,y,z}\frac{q_{\ell\beta}'^2+q_{\ell\gamma}'^2}{I_\alpha}\right]\frac{K(E,\boldsymbol{q})}{3N-6}\right\rangle, \tag{34}$$

where κ_ℓ is the kinetic energy of the ℓth atom.

Since $I_\alpha\sim Nr^2$ and $q_{\ell\beta}'^2<r^2$, where r is the radius of the cluster, the position dependent part in the right-hand side (rhs) of $\langle\kappa_\ell\rangle$ is less than $O(1/N)$ and so it vanishes in the thermodynamic limit. When fluctuation of an atom from its equilibrium position is very small, i.e., the cluster is in a solid state, then in Eq. (34) the $\boldsymbol{q}_\ell'$-dependent part does not fluctuate very significantly. Indeed, the fluctuation of $q_{\ell\beta}'^2/I_\alpha$ is estimated as

$$\delta(q^2/I) \simeq 2\frac{q}{I}\delta q+\frac{q^2}{I}\frac{\delta I}{I} \simeq 2\frac{qa}{I}\frac{\delta q}{a}+\frac{q^2}{I}N^{-1/3}\frac{\delta q}{a}, \tag{35}$$

where $\delta q/a$ is the ratio of the position fluctuation of an atom to the bond length, which is less than 0.1 in the solid phase, as is well known as the Lindemann index. Thus the relative fluctuation is small and the position dependent factors in Eq. (34) can be taken out of the average.

According to the numerical simulation discussed in Sec. II, we defined the local temperature of the ℓth atom by using its average kinetic energy: $T_\ell^\kappa=\frac{2\langle\kappa_\ell\rangle}{3k_B}$. Suppose that the cluster shape is approximately isotropic and so all the moments of inertia are nearly equal: $I=I_x\simeq I_y\simeq I_z$. Then local temperature can be regarded as a function of the ℓth atom's distance from the center of mass $r_\ell=\sqrt{q_{\ell x}'^2+q_{\ell y}'^2+q_{\ell z}'^2}$. It also depends on the mass of the atom,

$$T_\ell^\kappa = \left(1-\frac{m_\ell}{M}-\frac{2}{3}\frac{m\langle r_\ell\rangle^2}{\langle I\rangle}\right)T(E), \tag{36}$$

where the relation between thermodynamic temperature and total kinetic energy $T(E)=\frac{\langle 2K(E,\boldsymbol{q})\rangle}{(3N-6)k_B}$ was used [Eq. (28)]. From the above equation, when the system is a microcanonical ensemble whose total translational and angular momentum are zero, it is expected that the local kinetic temperature of an atom decreases as its distance from the center of mass increases. Detailed comparison with numerical results will be discussed in Sec. IV.

D. nth-order moment of kinetic energy of a particle

In Sec. III C we have derived the first-order moment of the kinetic energy of any atom, but it is insufficient for deriving the distribution function. In the present section, we demonstrate that a rigorous expression for the nth-order moment of the local kinetic energy, which has the information equivalent to the distribution function, can be derived. This is a generalization of Eq. (34).

Let $\boldsymbol{p}_\ell'={}^t(p_{\ell x}',p_{\ell y}',p_{\ell z}')$ be the momentum of the ℓth atom in the principal frame and $\boldsymbol{\xi}_\ell={}^t(\xi_7,\xi_8,\xi_9)$ be the new momentum corresponding to $\boldsymbol{p}_\ell'$ in the new frame. We again make use of formula (23) and average over the new momentum variables. To this end we take the submatrix of $\boldsymbol{T}(\boldsymbol{q}')$ containing only the relevant components, namely,

$$\boldsymbol{T}'(\boldsymbol{q}') = \begin{pmatrix} T_{77} & 0 & 0 \\ T_{87} & T_{88} & 0 \\ T_{97} & T_{98} & T_{99} \end{pmatrix}, \tag{37}$$

then the new momentum vector is related to the original momentum vectors as $\boldsymbol{p}_\ell=\boldsymbol{T}'(\boldsymbol{q}')\boldsymbol{\xi}_\ell$ because Eq. (14) holds and $\xi_1,\xi_2,\ldots,\xi_6$ can be taken as null according to the δ-functional distribution in Eq. (24).

Thus the kinetic energy of the ℓth atom is written as

$$\kappa_\ell = \tfrac{1}{2}{}^t\boldsymbol{\xi}_\ell\,\nu(\boldsymbol{q})\boldsymbol{\xi}_\ell, \tag{38}$$

where $\nu(\boldsymbol{q})={}^t\boldsymbol{T}'\,\boldsymbol{T}'$ is a 3×3 symmetric matrix.

Substituting the expression into Eq. (23) with $X(\boldsymbol{\xi}',\boldsymbol{q})=\kappa_\ell^n$ and $s=3$, we calculate the statistical average of the nth-order moment,

$$\langle\kappa_\ell^n\rangle = \frac{C_{N,3}}{2}\frac{\int d\boldsymbol{\xi}_\ell d\boldsymbol{q}({}^t\boldsymbol{\xi}_\ell\;\nu(\boldsymbol{q})\boldsymbol{\xi}_\ell)^n\hat{\sigma}(\boldsymbol{\xi}_\ell,\boldsymbol{q})/\sqrt{|I(\boldsymbol{q})|}}{\int d\boldsymbol{q}[2K(E,\boldsymbol{q})]^{(3N-8)/2}/\sqrt{|I(\boldsymbol{q})|}}, \tag{39}$$

where $\hat{\sigma}(\boldsymbol{\xi}_\ell,\boldsymbol{q})=[2K(E-\boldsymbol{\xi}_\ell^2/2,\boldsymbol{q})](3N-11)/2$ and $C_{N,3}=\frac{3N-9}{3N-6}\frac{\pi_{3N-9}}{\pi_{3N-6}}$. By introducing the orthogonal transformation $U:\boldsymbol{\xi}_\ell\to\boldsymbol{\xi}_\ell^*$ diagonalizing the matrix ν, the function $[{}^t\boldsymbol{\xi}_\ell\;\nu(\boldsymbol{q})\boldsymbol{\xi}_\ell]^n$ in the integrand is expressed as

$$\left(\sum_{i=7}^{9}\nu_i\xi_i^{*2}\right)^n=\sum_{n_7+n_8+n_9=n}\frac{n!}{n_7!\,n_8!\,n_9!}\prod_{i=7}^{9}\nu_i^{n_i}\xi_i^{*2n_i},\quad(40)$$

where ν_7, ν_8, and ν_9 are eigenvalues of the matrix $\nu(\boldsymbol{q})$. Substituting this into Eq. (B8) gives the nth moment of kinetic energy of the ℓ atom as

$$\langle\kappa_\ell^n\rangle=\sum_{n_7+n_8+n_9=n}\frac{n!}{n_7!\,n_8!\,n_9!}C_{N,3}\mathcal{D}(n_7,n_8,n_9)\times\left\langle\prod_{i=7}^{9}\nu_i(\boldsymbol{q})^{n_i}[2K(E,\boldsymbol{q})]^n\right\rangle,\quad(41)$$

where $\mathcal{D}(n_7,n_8,n_9)$ is a constant described in Appendix B. The angle brackets in the left-hand side are the statistical average defined by Eq. (26).

Equation (41) says that the nth moment $\langle\kappa_\ell^n\rangle$ can be described in terms of symmetrical polynomials of the eigenvalues ν_7, ν_8, and ν_9, which are all expressed by the three basic symmetrical polynomials $\nu_7+\nu_8+\nu_9$, $\nu_7\nu_8+\nu_8\nu_9+\nu_9\nu_7$, and $\nu_7\nu_8\nu_9$ for the cubic characteristic equation of the 3×3 matrix $\nu(\boldsymbol{q})$. The three basic symmetrical polynomials are, on the other hand, expressed in terms of the coefficients of the cubic equation depending explicitly on the coordinates of the atom. The coefficients can be calculated by the three successive Gram-Schmidt procedures of orthogonalization to obtain $\boldsymbol{e}_7$, $\boldsymbol{e}_8$, and $\boldsymbol{e}_9$, which are straightforward extensions of the task described in Sec. III C. The computation is tedious but straightforward. We thus only refer to the final result,

$$\nu_7+\nu_8+\nu_9=\sum_{\alpha=x,y,z}e_{\alpha\alpha},$$

$$\nu_7\nu_8+\nu_8\nu_9+\nu_9\nu_7=\frac{1}{2}\sum_{\alpha\neq\beta}(e_{\alpha\alpha}e_{\beta\beta}-e_{\alpha\beta}^2),$$

$$\nu_7\nu_8\nu_9=-2e_{xy}e_{yz}e_{zx}+e_{xx}e_{yy}e_{zz}-\sum_{\alpha\neq\beta\neq\gamma}\frac{e_{\alpha\alpha}e_{\beta\gamma}^2}{2}.$$

The parameters $e_{\alpha\beta}$ $(\alpha,\beta=x,y,z)$ are expressed in terms of the moment of inertia (which depends on all the components of $\boldsymbol{q}$) and the coordinates of the atom,

$$e_{\alpha\beta}=\delta_{\alpha\beta}+\Delta e_{\alpha\beta},\quad(42)$$

where

$$\Delta e_{\alpha\beta}\equiv\delta_{\alpha\beta}\left(-\frac{m_\ell}{M}-\frac{q_{\ell\beta}'^2}{I_\gamma}-\frac{q_{\ell\gamma}'^2}{I_\beta}\right)-(1-\delta_{\alpha\beta})\frac{q_{\ell\alpha}'q_{\ell\beta}'}{I_\gamma}\quad(43)$$

and $\delta_{\alpha\beta}$ is Kronecker's delta. For instance, it is easily shown that e_{xx} corresponds to Eq. (32).

One can readily check the first moment

$$\langle\kappa_\ell\rangle=\frac{\sum_{j=7}^{9}\langle\nu_j(\boldsymbol{q})2K(E,\boldsymbol{q})\rangle}{3(3N-6)}\quad(44)$$

reproducing the expression of Eq. (34).

As mentioned in Sec. III C, all the quantities such as $|q_{\ell\beta}^2/I_\gamma|$ and $|q_{\ell\beta}q_{\ell\alpha}/I_\gamma|$ in the rhs of the second equation are all less than $O(1/N)$ and $\Delta e_{\alpha\beta}$ is a quantity of $O(1/N)$, namely, $e_{\alpha\beta}$ is $\delta_{\alpha\beta}$ plus $\boldsymbol{q}_\ell$-dependent part of $O(1/N)$. Then from Eq. (42) one can easily prove that all the characteristic roots are approximately 1, and the deviation from it, which depends on the coordinate vector $\boldsymbol{q}$, is of $O(1/N)$,

$$\nu_i(\boldsymbol{q})=1+\Delta\nu_i(\boldsymbol{q}),\quad(45)$$

where $|\Delta\nu_i(\boldsymbol{q})|\simeq O(1/N)$.

E. Distribution function of local kinetic energy

The expressions obtained in Secs. III A–III D are rigorous but physically less intuitive. What we would like to know is whether or not the distribution function of local kinetic energy κ_ℓ really follows the Maxwell-Boltzmann distribution with the local temperature defined by $T_\ell^\kappa=\frac{2\langle\kappa_\ell\rangle}{3k_B}$. In this section we show that the distribution of the kinetic energy does follows the Maxwell-Boltzmann distribution under some approximation.

First the distribution function of κ_ℓ is given by

$$\rho(\kappa_\ell)=\langle\delta(\boldsymbol{p}_\ell'^2/2-\kappa_\ell)\rangle.\quad(46)$$

As has been done in Sec. III D [Eq. (38)], we transform the momentum $\boldsymbol{p}_\ell'$ into the new momentum variables $\boldsymbol{\xi}_\ell$; $\boldsymbol{p}_\ell'^2/2={}^t\boldsymbol{\xi}_\ell\,\nu(\boldsymbol{q})\boldsymbol{\xi}_\ell/2$, $[\boldsymbol{\xi}_\ell={}^t(\xi_7,\xi_8,\xi_9)]$. Then the statistical average in the rhs is computed by setting $X(\boldsymbol{q},\boldsymbol{\xi})=\delta({}^t\boldsymbol{\xi}_\ell\,\nu(\boldsymbol{q})\boldsymbol{\xi}_\ell/2-\kappa_\ell)$ in Eq. (23). Further, as in Sec. III D, making the transformation diagonalizing $\nu(\boldsymbol{q})$ with the orthogonal transformation $U:\boldsymbol{\xi}_\ell\to\boldsymbol{\xi}_\ell^*$ and introducing new momentum variables $\tilde{\xi}_i=\sqrt{\nu_i}\xi_i^*$, we are finally lead to the following expression:

$$\rho(\kappa_\ell)=C_{N,3}\frac{\int d\tilde{\boldsymbol{\xi}}_\ell\,\delta({}^t\tilde{\boldsymbol{\xi}}_\ell\tilde{\boldsymbol{\xi}}_\ell/2-\kappa_\ell)F(\tilde{\xi}_7^2,\tilde{\xi}_8^2,\tilde{\xi}_9^2)}{\int d\boldsymbol{q}[2K(E,\boldsymbol{q})]^{(3N-8)/2}/\sqrt{|I(\boldsymbol{q})|}}.\quad(47)$$

Here the function $F(\tilde{\xi}_7^2,\tilde{\xi}_8^2,\tilde{\xi}_9^2)$ is defined by

$$F(\tilde{\xi}_7^2,\tilde{\xi}_8^2,\tilde{\xi}_9^2)=\int d\boldsymbol{q}/\sqrt{|I(\boldsymbol{q})|}\prod_{j=7}^{9}\nu_i(\boldsymbol{q})^{-1/2}\times\left[2K\left(E-\sum_{j=7}^{9}\frac{\tilde{\xi}_i^2}{2\nu_i(\boldsymbol{q})},\boldsymbol{q}\right)\right]^{(3N-11)/2}.$$

To make further evaluation some approximation is inevitable. We here exponentialize the function $F(\tilde{\xi}_7^2,\tilde{\xi}_8^2,\tilde{\xi}_9^2)$ and apply the cumulant expansion

$$\log F(\tilde{\xi}_7^2,\tilde{\xi}_8^2,\tilde{\xi}_9^2)=\log F(0,0,0)+\sum_{i=7}^{9}\left.\frac{\partial F(\tilde{\xi}_7^2,\tilde{\xi}_8^2,\tilde{\xi}_9^2)/\partial\tilde{\xi}_i^2}{F(\tilde{\xi}_7^2,\tilde{\xi}_8^2,\tilde{\xi}_9^2)}\right|_{\tilde{\xi}_i^2=0}\tilde{\xi}_i^2+O(\tilde{\xi}_i^2\tilde{\xi}_j^2).\quad(48)$$

The approximation made here is to neglect terms of order

higher than quadratic terms. The cumulant expansion is roughly a system size expansion, and this approximation means to neglect all the terms less than or equal to $O(1/N)$.

The coefficient of the lowest order term $\tilde{\xi}_i^2$ is given by

$$-\frac{3N-11}{2}\frac{\int \frac{d\boldsymbol{q}}{\sqrt{|I(\boldsymbol{q})|}}\prod_{j=7}^{9}\nu_j(\boldsymbol{q})^{-1/2}\nu_i(\boldsymbol{q})^{-1}[2K(E,\boldsymbol{q})]^{(3N-13)/2}}{\int \frac{d\boldsymbol{q}}{\sqrt{|I(\boldsymbol{q})|}}\prod_{j=7}^{9}\nu_j(\boldsymbol{q})^{-1/2}[2K(E,\boldsymbol{q})]^{(3N-11)/2}}.$$

In order to apply Eq. (26), we divide both the numerator and denominator by $\int d\boldsymbol{q}/\sqrt{|I(\boldsymbol{q})|}[2K(E,\boldsymbol{q})]^{(3N-8)/2}$. Then the lowest order cumulant expansion leads to the following result:

$$\rho(\kappa_\ell) \propto \int d\tilde{\boldsymbol{\xi}}_\ell \delta(\kappa_\ell - \tilde{\boldsymbol{\xi}}_\ell^2/2)\exp\left[-\sum_{j=7}^{9}\alpha_j\tilde{\xi}_j^2\right], \tag{49}$$

where the coefficient α_i, which comes from the coefficient Eq. (49), is

$$\alpha_i = \frac{3N-11}{2}\frac{\left\langle \prod_{j=7}^{9}\nu_j(\boldsymbol{q})^{-1/2}\nu_i(\boldsymbol{q})^{-1}[2K(E,\boldsymbol{q})]^{-5/2}\right\rangle}{\left\langle \prod_{j=7}^{9}\nu_j(\boldsymbol{q})^{-1/2}[2K(E,\boldsymbol{q})]^{-3/2}\right\rangle}. \tag{50}$$

The integration over $\tilde{\xi}_i$ is done by using the polar coordinate

$$\rho(\kappa_\ell) \propto \sqrt{\kappa_\ell}e^{-(\alpha_1+\alpha_2)\kappa_\ell}\int_0^1 dx \mathrm{e}^{(\alpha_1+\alpha_2-2\alpha_3)\kappa_\ell x^2} I_0 \times[\kappa_\ell(|\alpha_1-\alpha_2|)(1-x^2)], \tag{51}$$

where $I_0(z)$ is zeroth-order modified Bessel function: $I_0(z) = \frac{1}{2\pi}\int_0^{2\pi}\exp(z\cos 2\varphi)d\varphi$.

Let us introduce the harmonic average of $2\alpha_i$ as

$$\frac{1}{\alpha} \equiv \frac{1}{3}\sum_{j=7}^{9}\frac{1}{2\alpha_j}. \tag{52}$$

In the energy regime of κ_ℓ such that $\kappa_\ell\alpha < O(1)$ where the distribution has a significant weight, the distribution function is expanded by the smallness parameter $|\alpha_i-\alpha_j|/\alpha \simeq |\nu_i-\nu_j| \simeq O(1/N)$ [see Eqs. (45) and (50)],

$$\rho(\kappa_\ell) \propto \sqrt{\kappa_\ell}\mathrm{e}^{-\alpha\kappa_\ell}\left[1+\left(-\frac{2\kappa_\ell\alpha}{9}+\frac{2\kappa_\ell^2\alpha^2}{45}\right)\sum_{i\neq j}\frac{(\alpha_i-\alpha_j)^2}{\alpha^2} + O\left(\frac{(\alpha_i-\alpha_j)^3}{\alpha^3}\right)\right]. \tag{53}$$

The above expression suggests that the distribution function deviates from the Maxwell-Boltzmann distribution. But the coefficient of the correction term, which is proportional to $(|\alpha_i-\alpha_j|/\alpha)^2 \simeq |\nu_i-\nu_j|^2 \simeq O(1/N^2)$, is very small. We can thus neglect the correction terms, and the distribution function is well approximated by the Maxwell-Boltzmann distribution,

$$\rho(\kappa_\ell) \propto \sqrt{\kappa_\ell}\mathrm{e}^{-\kappa_\ell/k_B\tilde{T}_\ell^{\mathrm{MB}}} \tag{54}$$

with the local MB temperature

$$\tilde{T}_\ell^{\mathrm{MB}} = \frac{1}{3(3N-11)k_B}\times\sum_{i=7}^{9}\frac{\left\langle \prod_{j=7}^{9}\nu_j(\boldsymbol{q})^{-1/2}[2K(E,\boldsymbol{q})]^{-3/2}\right\rangle}{\left\langle \prod_{j=7}^{9}\nu_j(\boldsymbol{q})^{-1/2}\nu_i(\boldsymbol{q})^{-1}[2K(E,\boldsymbol{q})]^{-5/2}\right\rangle}. \tag{55}$$

This expression is seemingly rather different from the rigorous expression for the local kinetic temperature defined by Eq. (4) with Eq. (44) or (34) on the basis of the average kinetic energy.

This is, of course, due to the approximations applied so far. However, as shown below, these two expressions coincide if N is large enough. For brevity, let us denote the factors $\nu_i(\boldsymbol{q})$ and $\Pi_{j=7}^{9}\nu_j(\boldsymbol{q})^{-1/2}\nu_i(\boldsymbol{q})^{-1}$ in Eq. (55) by $X(\boldsymbol{q})$ and $Y(\boldsymbol{q})$, respectively. Then the numerator in the rhs of Eq. (55) can be expressed by $\langle(2K)^{-3/2}XY\rangle$. If the factorization $\langle(2K)^{-3/2}XY\rangle = \langle(2K)^{-5/2}Y\times 2KX\rangle \simeq \langle(2K)^{-5/2}Y\rangle\langle 2KX\rangle$ is allowed, Eq. (55) coincides with Eq. (4) with Eq. (44) [or Eq. (34)] and T_ℓ^κ can be identified with $\tilde{T}_\ell^{\mathrm{MB}}$. We, therefore, evaluate the deviation of the ratio of the two quantities from unity,

$$\Delta \equiv \frac{\langle[2K(\boldsymbol{q})]^{-3/2}X(\boldsymbol{q})Y(\boldsymbol{q})\rangle}{\langle[2K(\boldsymbol{q})]^{-5/2}Y(\boldsymbol{q})\rangle\langle 2K(\boldsymbol{q})X(\boldsymbol{q})\rangle} - 1, \tag{56}$$

where $K(\boldsymbol{q}) = K(E,\boldsymbol{q})$. We separate each quantity into its statistical average and the deviation from the average,

$$K(\boldsymbol{q}) = \langle K\rangle + \delta K(\boldsymbol{q})$$

$$X(\boldsymbol{q}) = \langle X\rangle + \delta X(\boldsymbol{q})$$

$$Y(\boldsymbol{q}) = \langle Y\rangle + \delta Y(\boldsymbol{q}). \tag{57}$$

It should be noted that, by the definition and Eq. (45), $\langle X\rangle$ and $\langle Y\rangle$ may both depend on the position $\boldsymbol{q}_\ell$ of the ℓth atom but they are both nearly 1, and $\delta X(\boldsymbol{q})$ and $\delta Y(\boldsymbol{q})$ are of $O(1/N)$, whereas $\langle K\rangle$ is the average of the total kinetic energy and independent of $\boldsymbol{q}_\ell$. Substituting Eq. (57) into Eq. (56) and expanding into the powers of $k = \delta K/\langle K\rangle$, $x = \delta X/\langle X\rangle$, and $y = \delta Y/\langle Y\rangle$, Eq. (56) is estimated as

$$\Delta \simeq -\tfrac{5}{2}\langle k^2\rangle - \tfrac{5}{2}\langle kx\rangle + \langle ky\rangle + \langle xy\rangle. \tag{58}$$

Since $\langle k^2\rangle = \frac{\langle\delta K^2\rangle}{\langle K\rangle^2} \simeq O(1/N)$ and $|x| = \frac{|\delta X|}{\langle X\rangle} < O(1/N)$, the largest order contribution comes from the first term of the rhs, which does not depend on $\boldsymbol{q}_\ell$. In particular, since we assume the fluctuations are small, i.e., in solid phase, x and y are extremely small as $x \simeq \frac{q^2}{I}N^{-1/3}\frac{\delta q}{a} \simeq N^{-4/3}\frac{\delta q}{a}$ according to the estimation of Eq. (35). Consequently, up to the correction of $O(1/N)$, the ratio of the two temperatures is a constant independent of the position of the ℓth atom,

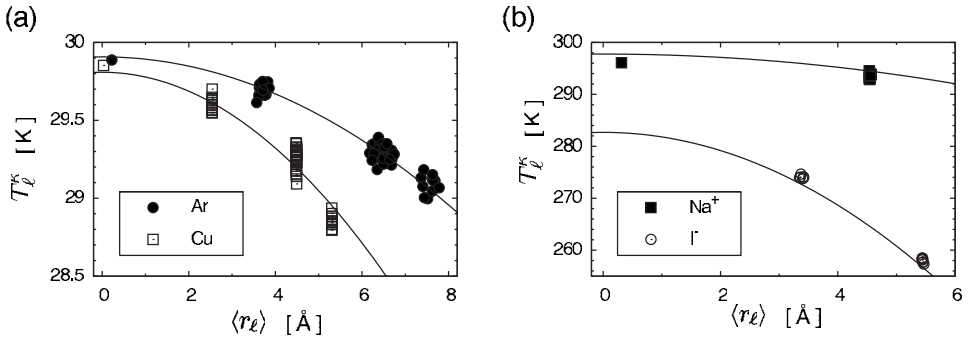

FIG. 6. The local temperature T_ℓ^κ of each individual atom as a function of the average distance from the center of mass $\langle r_\ell \rangle$ and the theoretical curves [Eq. (60)]. (a) Cu_{55} and Ar_{55}. (b) $(NaI)_{13}I^-$.

$$\frac{\tilde{T}_\ell^{\mathrm{MB}}}{T_\ell^\kappa} \simeq \frac{3N-6}{3N-11}\left(1-\frac{5}{2}\left\langle\frac{(K-\langle K\rangle)^2}{\langle K\rangle^2}\right\rangle\right), \tag{59}$$

which is very close to 1. Thus we have proved that the distribution function of the kinetic energy of a single particle is the Maxwell-Boltzmann distribution characterized by the local effective temperature $\tilde{T}_\ell^{\mathrm{MB}}$ which can be identified with T_ℓ^κ.

IV. DISCUSSION

In this section, by comparing the numerical results presented in Sec. II with the analytical evaluation in Sec. III, we conclude that inhomogeneity of local temperature in microclusters can be explained as a property of a microcanonical ensemble whose total translational and angular momentum are conserved. Then we give an intuitive interpretation for the origin of inhomogeneity in the local temperature, which makes the role of the momentum conservation more clear.

A. Comparison of numerical results and analytical evaluation

Returning to original coordinates from mass-weighted ones, the local temperature [Eq. (36)] is rewritten as

$$T_\ell^\kappa = \left(1-\frac{m_\ell}{M}-\frac{2}{3}\frac{m_\ell\langle r_\ell\rangle^2}{\langle I\rangle}\right)T(E). \tag{60}$$

This equation explains the decrease in T_ℓ^κ depending on the atomic mass m_ℓ and distance from the center of mass $\langle r_\ell \rangle$.

First of all, we consider clusters consisting of a single species of atoms. The numerical experiments corresponding to this situation are shown for Ar_{55} and Cu_{55} clusters in Sec. II [Fig. 3(b)], which are both set to the same thermodynamic temperature $T(E)$. The theoretical curves and the numerical results are compared in Fig. 6(a), which shows a nice agreement between the theoretical and numerical results.

The second term of the equation $-m_\ell/M=-1/N$ is common for Ar_{55} and Cu_{55} clusters, and therefore the local temperatures of the atoms at the centers of the clusters Ar_{55} and Cu_{55} are very close at the same thermodynamic temperature. The third term of the equation explains the decrease in local temperature with increase in the distance from the center. The rate of decrease is controlled by the factor

$$\frac{m_\ell}{\langle I\rangle} = \frac{3}{2}\left(\sum_{i=1}^{N} r_i^2\right)^{-1}, \tag{61}$$

which is determined by the size of the clusters if they have similar structure and consist of the same number of atoms. Ar_{55} and Cu_{55} clusters considered here have the same icosahedral structure, and the radius of the former cluster is larger than the latter one, and so the above ratio is smaller in the former cluster. This is the reason why the theoretical curve of local temperature of Cu_{55} decreases more rapidly than that of Ar_{55}.

Second, we consider clusters which consist of different species of atoms with different masses. In our study, we have employed an alkali halide cluster as a binary cluster system in Sec. II. Figure 6(b) shows a comparison between the numerical result and theoretical curves of $(NaI)_{13}I^-$ cluster, where the black squares and the white circles represent Na^+ and I^- atoms, respectively. In the figure, the agreement is quite good even in such a binary system. In a binary system, the theoretical curve splits into two curves because the second and the third terms of Eq. (60) contribute differently depending on the mass of the particle. Thus the local temperature exhibits different dependence on the distance for different species of atoms. In the simulation presented here, the masses of Na^+ and I^- are $m_{\mathrm{Na}}=22.99$ u and $m_{\mathrm{I}}=126.9$ u, respectively. I^- is about five times heavier than Na^+. Therefore the local temperature of Na^+ is higher than that of I^- at the center because of the difference in the second term. The decreasing rate of local temperature, which is controlled by the third term, is five times larger for I^- atoms than for Na^+ atoms. The numerical results in Fig. 6(b) exactly follow the above expectation: the local temperature of the heavier atom (I^-) drops more rapidly than that of the lighter one (Na^+).

Finally, the theoretical result of local temperature [Eq. (60)] shows that the inhomogeneity of local temperatures depends on the number of atoms in the cluster. Indeed, the second and third terms of the equation decrease in inverse proportion to N. Therefore, the inhomogeneity of the local temperature disappears in the thermodynamic limit $N\to\infty$, as has been stressed in Sec. III.

In fact, numerical results support this expectation: the decreasing rate of local temperature in $N=125[(NaI)_{62}I^-]$ or $N=147(Cu_{147})$ clusters is less noticeable than that of $N=27[(NaI)_{13}I^-]$ and $N=55(Cu_{55})$. The numerical results and theoretical evaluation are shown in Fig. 7, which confirms

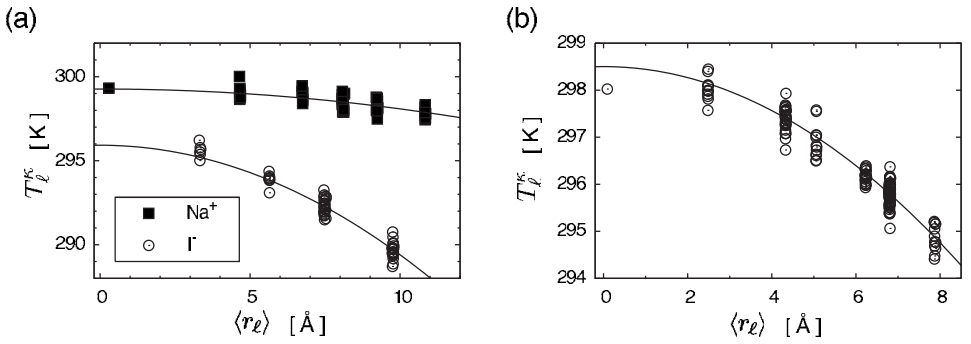

FIG. 7. The local temperature T_ℓ^κ of each individual atom as a function of distance from the center of mass $\langle r_\ell \rangle$ and the theoretical curves [Eq. (60)]. (a) $(NaI)_{62}I^-$ (N=125). (b) Cu_{147}.

that the theoretical prediction reproduces the dependency of the inhomogeneity in the local temperature on the total number of particles.

Thus we have confirmed that the inhomogeneity of the local temperature is caused by the conservation of total translational and angular momentum. This is, of course, consistent with the numerically observed fact that the inhomogeneity disappears when these quantities are not conserved after adding an anisotropic trap potential in Sec. II E. Smallness of the system emphasizes the effect of conserved quantities, making it possible to observe the inhomogeneity in the local temperatures of the individual atoms.

Finally, we refer and apply our result to Jellinek-Goldberg work [25]. Jellinek and Goldberg [25] introduced dynamical degrees of freedom f_ℓ which can be described by the theoretical evaluation of local temperature: $\frac{f_k}{N_k}=(1-\frac{m_k}{M}-\frac{2}{3}\frac{m_k\langle r_k\rangle^2}{\langle I\rangle})\frac{3(3N-8)}{3N-6}$, where f_k and N_k are dynamical degrees of freedom and the number of particles belonging to kth shell of the cluster and m_k and r_k are mass and distance from the center of mass of one of the atoms belonging to kth shell. We note that our evaluation gives good agreement with the numerical results by Jellinek and Goldberg [25], where average inertia moments of the clusters were obtained by numerical experiments with a many-body Gupta-type potential and used for theoretical evaluation: $\langle I\rangle \simeq 1.56\times 10^3$ u Å^2 for $(Al)_{13}$ and 1.98×10^4 u Å^2 for $(Al)_{55}$. Hence our result can explain their results.

B. Intuitive interpretation of inhomogeneous local temperature

In this section, we derive Eq. (34) [or Eq. (60)] by a very heuristic argument supposing that a cluster is in solid phase.

First of all, we consider the cluster as an N-particle ergodic system in which total translational and angular momentum are not conserved. Then the total kinetic energy of the system K' is equally distributed among all the particles and all degrees of freedom according to the standard equipartition rule, and the kinetic energy per 1 degree of freedom and the kinetic energy per particle are $K'/3N$ and K'/N, respectively, by the equipartition theorem.

The kinetic energy possessed by ℓth atom κ_ℓ is the sum of atomic vibrational energy κ_ℓ^V, overall translational energy κ_ℓ^G, and overall rotational energy κ_ℓ^R: $\kappa_\ell^G+\kappa_\ell^R+\kappa_\ell^V=\frac{K'}{N}$. On the contrary, if the total translational and angular momentum are conserved the ℓth atom energy consists only of vibrational energy, that is,

$$\kappa_\ell = \frac{K'}{N} - \kappa_\ell^G - \kappa_\ell^R. \tag{62}$$

We first consider the energy distributed to the rotational motion, which can be decomposed into the rotational motions around the three principal axes of the moment of inertia. Each of the 3 rotational degrees of freedom has the average kinetic energy $K'/3N$, respectively. Let Ω be the angular frequency of the whole rotational motion of the cluster, then the average kinetic energies of each component should be given by $\frac{I_\alpha}{2}\Omega_\alpha^2=K'/3N$. In this rotational motion the rotational kinetic energy distributed to a particle is $\kappa_\ell^R=\frac{1}{2}(I_{\ell x}\Omega_x^2+I_{\ell y}\Omega_y^2+I_{\ell z}\Omega_z^2)$, where $I_{\ell\alpha}$ is the moment of inertia around the principal axis α contributed by the ℓth particle, and it is given by $m_\ell(q_{\ell\beta}'^2+q_{\ell\gamma}'^2)$. From all the above relations, the overall rotational energy distributed to the ℓth particle is

$$\kappa_\ell^R = \frac{m_\ell}{3}\sum_{\alpha\neq\beta\neq\gamma}\frac{q_{\ell\beta}'^2+q_{\ell\gamma}'^2}{I_\alpha}\frac{K'}{N}. \tag{63}$$

A similar argument holds also for the overall translational energy. It is obvious that the translational energy distributed to the ℓth particle is

$$\kappa_\ell^G = m_\ell/M \times K'/N. \tag{64}$$

Substituting Eqs. (63) and (64) for Eq. (62), we get

$$\kappa_\ell = \left(1-\frac{m_\ell}{M}-\frac{m_\ell}{3}\sum_{\alpha,\beta,\gamma}\frac{\beta_\ell^2+\gamma_\ell^2}{I_\alpha}\right)\frac{K'}{N}. \tag{65}$$

Finally, we replace the total kinetic energy K' with K, the kinetic energy of the system for which the translational and rotational motions are frozen. Since the kinetic energy distributed to 1 degree of freedom is equal the relation $K/(3N-6)=K'/3N$ should hold. Then Eq. (65) essentially agrees with the rigorous expression for the kinetic energy represented by Eq. (34). The above argument shows us that the second and third terms in theoretical evaluation [Eq. (60) or (65)] obviously result from freezing of the overall translational and rotational motions, respectively.

In this paper, we considered only isolated clusters, i.e., systems under free boundary condition; however the above argument gives some expectations as follows. First, even for a system under periodic boundary condition, total translational momentum is still conserved so the effect of the second term which has mass dependence remains if the number of particles in the supercell of the periodic condition is small

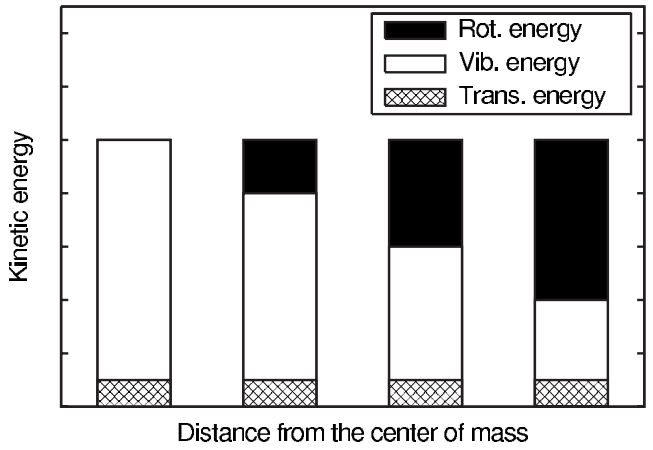

FIG. 8. Conceptual figure of kinetic energy distribution when the cluster consists of a single species of particle and kinetic energy is distributed among all particles equally. Each bar shows the distribution of the kinetic energy of the corresponding particle into its rotational energy κ_ℓ^R (black region), vibrational energy κ_ℓ^V (white region), and translational energy κ_ℓ^G (mesh region).

enough. Second, in Sec. III our evaluation is only for the systems whose total translational momentum $\boldsymbol{P}_0$ and rotational momentum $\boldsymbol{L}_0$ are equal to zero, i.e., $\kappa_\ell^G=\kappa_\ell^R=0$. However, even if $\kappa_\ell^G\neq 0$ or $\kappa_\ell^R\neq 0$, our evaluation can be easily extended if $\boldsymbol{P}_0$ and $\boldsymbol{L}_0$ are small enough. Finally, we assumed that clusters are in solid state implicitly in the above derivation. If the cluster is in liquid state, frequent exchange of position of particles results in vanishing of the third-term effect containing position dependence, but the second term with no position dependence does not disappear.

If all the degrees of freedom are active the kinetic energies distributed to individual particles are equal, but when the collective degrees of freedom contributing to the total translational and/or rotational motion are frozen, the kinetic energies of individual particles become inhomogeneous because the contributions from such macroscopic degrees of freedom to the kinetic energy, which depend on the position and mass of each particle according to Eqs. (63) and (64), are missing (see Fig. 8). Such missing energy is inversely proportional to the number of particles and is significant only in systems consisting of small number of particles.

We stress that the above argument only conventionally explains the kinetic energy distributed to each particle, but it does not explain why the distribution function of kinetic energy obeys the Maxwell-Boltzmann distribution characterized by a temperature related to the local kinetic energy.

V. CONCLUSION

In this paper, we showed that dynamical conserved quantities cause inhomogeneous kinetic energy distribution in microcanonical ensemble for a system composed of a small number of particles with conservation of total translational and angular momentum using MD simulations of microclusters and theoretical analysis of statistical mechanical properties of the ensemble.

In constant energy MD simulations of isolated cluster systems with archetypal two body interaction potential, Lennard-Jones potential (as Ar clusters), Morse potential (as Cu clusters) with icosahedral structures, and Coulomb potential [as $(\mathrm{NaI})_n$ clusters] with rocksalt-type structures, we showed that local temperatures, i.e., the kinetic energies distributed to each atom, can be inhomogeneous even when the kinetic energies of all particles fit the Maxwell-Boltzmann distribution, i.e., the system is in thermal equilibrium. The numerical results revealed that the local temperature depends on the mass and distance of each atom from the center of mass. Specifically, the temperature of a particle decreases with increase in its distance from the center of mass, and the temperature of a heavier particle is less than that of a lighter one in a binary component cluster containing different mass particles, e.g., alkali halide cluster. These behaviors are suppressed as the number of particles of the system increases.

For analysis of these behaviors, we evaluated statistical average of kinetic energy distributed to individual particle [Eq. (36)] and deduced approximately the distribution function of the energy [Eqs. (54) and (55)] based on statistical mechanics of microcanonical ensemble with conservation of total translational and angular momentum. The agreement between the theoretical evaluation of the average kinetic energy and the numerical results was quite good. Therefore we concluded that the inhomogeneity of local temperature is caused by the existence of the conserved quantities, total translational, and angular momentum. It is not dependent on the type of the interactions between the particles but depends on the translational and rotational symmetries of the system.

ACKNOWLEDGMENTS

This work was supported by Grant-in-Aid for JSPS Fellows (KAKENHI) from the Ministry of Education. The authors are grateful to S. Tsuji for his hospitality.

APPENDIX A

Consider the integral with respect to a mass-weighted momentum ξ_i,

$$B=\int \xi_i^2\{2[K(E,\boldsymbol{q})-\xi_i^2/2]\}^{D/2}d\xi_i, \tag{A1}$$

where $K(E,\boldsymbol{q})=E-V(\boldsymbol{q})$ is the total kinetic energy of a system. Since the kinetic energy of a degree of freedom $\xi_i^2/2$ is less than the total kinetic energy, the integral domain is from $-\sqrt{2K}$ to $\sqrt{2K}$. Now we define the new momentum as $\xi_i^*=\xi_i/\sqrt{2K(E,\boldsymbol{q})}$, then the integration is given by

$$B=[2K(E,\boldsymbol{q})]^{(D+3)/2}2\int_0^1 \xi_i^{*2}(1-\xi_i^{*2})^{D/2}d\xi_i^*. \tag{A2}$$

The integration on the right-hand side is described by a beta function: $\int_0^1\xi_i^{*2}(1-\xi_i^{*2})^{D/2}d\xi_i^*=B(3/2,D/2+1)/2=\frac{1}{2(D+2)}\frac{\pi_{D+3}}{\pi_{D+2}}$. Therefore we can integrate it and get the relation

$$\int \xi_i^2[2K(E-\xi_i^2/2,\boldsymbol{q})]^{D/2}d\xi_i=\frac{1}{D+2}\frac{\pi_{D+3}}{\pi_{D+2}}[2K(\boldsymbol{q})]^{(D+3)/2}. \tag{A3}$$

APPENDIX B

We consider the integration

$$A = \int \theta\left(R(\boldsymbol{q}) - \sum_{i=7}^{9} a_i \xi_i^2/2 - \sum_{i\neq 7,8,9}^{M+3} \xi_i^2/2 \right) A(\boldsymbol{q}) d\boldsymbol{q} d\xi, \tag{B1}$$

where $A(\boldsymbol{q})$ and $R(\boldsymbol{q})$ are arbitrary functions of coordinate variables $\boldsymbol{q}$.

First, we take new momentum variables: $\xi_k' = \sqrt{a_k/2R(\boldsymbol{q})}\xi_k (k=7,8,9)$, $\xi_k' = \xi_k/\sqrt{2R(\boldsymbol{q})}$ $(k=1,2,\ldots,M+3; k\neq 7,8,9)$, then the above step function takes the form $\theta[R(\boldsymbol{q}) - \Sigma \xi_i'^2/2]$. Thus, we can integrate the equation over $\boldsymbol{\xi}'$ and obtain

$$A = (a_7 a_8 a_9)^{-1/2} \pi_{M+3} \int A(\boldsymbol{q}) [2R(\boldsymbol{q})]^{(M+3)/2} d\boldsymbol{q}, \tag{B2}$$

where π_M is the volume of a M-dimensional unit super sphere. After n_7, n_8, and n_9 times differentiation of the equation with respect to a_7, a_8, and a_9, respectively, gives

$$\frac{\partial^{n_7+n_8+n_9}}{\partial a_7^{n_7}\, \partial a_8^{n_8}\, \partial a_9^{n_9}} A = \prod_{i=7}^{9} (-1)^{n_i} (n_i - 1 + 1/2)!\, \pi_{M+3} \int A(\boldsymbol{q}) \times [2R(\boldsymbol{q})]^{(M+3)/2} d\boldsymbol{q}. \tag{B3}$$

Here we use the relation, $(-\frac{1}{2})(-\frac{1}{2}-1)\cdots(-\frac{1}{2}-n_i+1) = (-1)^{n_i}(n_i-1+1/2)!$.

On the other hand, for Eq. (B1) the transformation $\xi_i' = \xi_i/\sqrt{2R(\boldsymbol{q}) - (a_7\xi_7^2 + a_8\xi_8^2 + a_9\xi_9^2)}$ $(i=1,\ldots,M+3; i\neq 7,8,9)$ can be decomposed into a step function depending only on the momentum variables ξ_i' and a part depending on the other momenta ξ_7, ξ_8, and ξ_9 and coordinate variables $\boldsymbol{q}$. Therefore, we can integrate over ξ_i' and obtain

$$A = \pi_M \int A(\boldsymbol{q}) \left[2\left(R(\boldsymbol{q}) - \sum_{i=7}^{9} a_i \xi_i^2/2 \right) \right]^{M/2} d\xi_7 d\xi_8 d\xi_9 d\boldsymbol{q}. \tag{B4}$$

Similarly as above, n_7, n_8, and n_9 times differentiation of the equation with respect to a_7, a_8, and a_9, respectively, gives

$$\frac{\partial^{n_7+n_8+n_9}}{\partial a_7^{n_7}\, \partial a_8^{n_8}\, \partial a_9^{n_9}} A = \frac{(M/2)!}{(n_7+n_8+n_9)!} \pi_M \int A(\boldsymbol{q}) \times \left[2\left(R(\boldsymbol{q}) - \sum_{i=7}^{9} \frac{a_i \xi_i^2}{2} \right) \right]^{M/2-n_7-n_8-n_9} \times \prod_{i=7}^{9} (-1)^{n_i} \xi_i^{2n_i} d\xi_i d\boldsymbol{q}. \tag{B5}$$

Now substituting $a_7=a_8=a_9=1$ and $M/2-n_1-n_2-n_3 = M'/2$ into Eqs. (B3) and (B5) gives

$$\int A(\boldsymbol{q}) \left[2\left(R(\boldsymbol{q}) - \sum_{i=7}^{9} \xi_i^2/2 \right) \right]^{M'/2} \prod_{i=7}^{9} \xi_i^{2n_i} d\xi_i d\boldsymbol{q} = \mathcal{D}(n_7,n_8,n_9) \int [2(R\ (\boldsymbol{q})]^{(M'+3)/2+n} A(\boldsymbol{q}) d\boldsymbol{q}, \tag{B6}$$

where $n_7+n_8+n_9=n$ and

$$\mathcal{D}(n_7,n_8,n_9) = \prod_{k=7}^{9} (n_k - 1 + 1/2)!\, \frac{\pi_{M'+2n+3}}{\pi_{M'+2n}} \frac{(M'/2)!}{(M'/2+n)!}. \tag{B7}$$

If we consider $A(\boldsymbol{q}) = \Pi_{i=7}^{9} \nu_i(\boldsymbol{q})^{n_i}/\sqrt{I(\boldsymbol{q})}$, substitute this into Eq. (B6) and divide the equation by $\int [2R(\boldsymbol{q})]^{(M'+3)/2} d\boldsymbol{q}/\sqrt{|I(\boldsymbol{q})|}$, then the right-hand side integral becomes the phase space average: $\langle \Pi_{i=7}^{9} \nu_i^{n_i} [2R(\boldsymbol{q})]^n \rangle$. Finally, let $R(\boldsymbol{q}) = E - V(\boldsymbol{q})$ and $M' = 3N-11$, then we obtain the relation

$$\frac{\int \prod_{i=7}^{9} \nu_i^{n_i} \xi_i^{2n_i} [2(E - V(\boldsymbol{q}) - \boldsymbol{\xi}_\ell^2/2)]^{(3N-11)/2} d\boldsymbol{\xi}_\ell d\boldsymbol{q}/\sqrt{|I(\boldsymbol{q})|}}{\int [2E - V(\boldsymbol{q})]^{(3N-8)/2} d\boldsymbol{q}/\sqrt{|I(\boldsymbol{q})|}} = \mathcal{D}(n_7,n_8,n_9) \left\langle \prod_{i=7}^{9} \nu_i^{n_i} [2(E - V(\boldsymbol{q}))]^n \right\rangle, \tag{B8}$$

where $\mathcal{D}(n_7,n_8,n_9) = \Pi_{k=7}^{9} (n_k - 1 + 1/2)!\, \frac{\pi_{3N-8+2n}}{\pi_{3N-11+2n}} \frac{[(3N-11)/2]!}{[(3N-11)/2+n]!}$.

[1] Ph. Buffat and J.-P. Borel, Phys. Rev. A **13**, 2287 (1976).
[2] J. Bovin, R. Wallenberg, and D. Smith, Nature (London) **317**, 47 (1985).
[3] S. Iijima and T. Ichihashi, Phys. Rev. Lett. **56**, 616 (1986).
[4] M. Mitome, Y. Tanishiro, and K. Takayanagi, Z. Phys. D: At., Mol. Clusters **12**, 45 (1989).
[5] P. M. Ajayan and L. D. Marks, Phys. Rev. Lett. **63**, 279 (1989).
[6] S. Sawada and S. Sugano, Z. Phys. D: At., Mol. Clusters **14**, 247 (1989).
[7] M. Schmidt, R. Kusche, T. Hippler, J. Donges, W. Kronmüller, B. von Issendorff, and H. Haberland, Phys. Rev. Lett. **86**, 1191 (2001).
[8] F. Gobet, B. Farizon, M. Farizon, M. J. Gaillard, J. P. Buchet, M. Carre, P. Scheier, and T. D. Mark, Phys. Rev. Lett. **89**, 183403 (2002).
[9] H. A. Posch and W. Thirring, Phys. Rev. Lett. **95**, 251101 (2005).
[10] H. Yasuda and H. Mori, Z. Phys. D: At., Mol. Clusters **31**, 131 (1994).
[11] H. Yasuda, H. Mori, M. Komatsu, K. Takeda, and H. Fujita, J. Electron Microsc. **41**, 267 (1992).
[12] H. Yasuda and H. Mori, Phys. Rev. Lett. **69**, 3747 (1992).
[13] Y. Shimizu, S. Sawada, and K. Ikeda, Eur. Phys. J. D **4**, 365 (1998).
[14] Y. Shimizu, K. S. Ikeda, and S. I. Sawada, Phys. Rev. B **64**,

075412 (2001).
[15] D. J. Wales and R. S. Berry, Phys. Rev. Lett. **73**, 2875 (1994).
[16] G. A. Breaux, C. M. Neal, B. Cao, and M. F. Jarrold, Phys. Rev. Lett. **94**, 173401 (2005).
[17] S. Pochon, K. F. MacDonald, R. J. Knize, and N. I. Zheludev, Phys. Rev. Lett. **92**, 145702 (2004).
[18] E. Fermi, J. Pasta, and S. Ulam, Los Alalmos Science Laboratory Report No. LA-1940, 1955.
[19] J. Jellinek, T. L. Beck, and R. S. Berry, J. Chem. Phys. **84**, 2783 (1986).
[20] G. Nyman, S. Nordholm, and H. Schranz, J. Chem. Phys. **93**, 6767 (1990).
[21] R. Dumont, J. Chem. Phys. **95**, 9172 (1991).
[22] R. Dumont, J. Chem. Phys. **96**, 2203 (1992).
[23] T. Niiyama, Y. Shimizu, T. R. Kobayashi, T. Okushima, and K. S. Ikeda, Phys. Rev. Lett. **99**, 014102 (2007).
[24] M. Allen and D. Tildesley, *Computer Simulation of Liquids* (Oxford University Press, New York, 1989).
[25] J. Jellinek and A. Goldberg, J. Chem. Phys. **113**, 2570 (2000).
[26] U. Salian, J. Chem. Phys. **108**, 6342 (1998).
[27] J. P. K. Doye and D. J. Wales, Phys. Rev. B **59**, 2292 (1999).
[28] D. J. Wales, *Energy Landscapes* (Cambridge University Press, Cambridge, 2003).
[29] J. Lennard-Jones, Proc. Phys. Soc. London **43**, 461 (1931).
[30] P. Morse, Phys. Rev. **34**, 57 (1929).
[31] L. A. Girifalco and V. G. Weizer, Phys. Rev. **114**, 687 (1959).
[32] M. Born and J. Mayer, Z. Phys A, Hadrons Nucl. **75**, 1 (1932).
[33] F. Fumi and M. Tosi, J. Phys. Chem. Solids **25**, 31 (1964).
[34] M. Tosi and F. Fumi, J. Phys. Chem. Solids **25**, 45 (1964).
[35] It should be noted that we refer to the system "ergodic" when the system can visit with uniform probability the whole constant energy surface under the constraint of the total translational and angular momentum conservation. Needless to say, if the total translational and angular momentum are not conserved in the system, we use the word ergodic in the more general sense.
[36] E. M. Pearson, T. Halicioglu, and W. A. Tiller, Phys. Rev. A **32**, 3030 (1985).
[37] F. Calvo and P. Labastie, Eur. Phys. J. D **3**, 229 (1998).